AD-A115 101 MINNESOTA UNIV MINNEAPOLIS DEPT OF AEROSPACE ENGINE--ETC F/G 13/13
STRUCTURAL INELASTICITY. XXVIII.(U)
MAR 82 P G HODGE, P TAIT, J MALONE N00014-75-C-0177
UNCLASSIFIED AEM-H1-28 NL

END
DATE
FILMED
7 82
DTIC

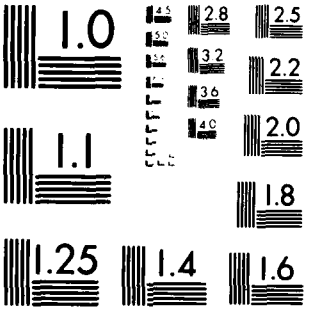

MICROCOPY RESOLUTION TEST CHART
NATIONAL BUREAU OF STANDARDS 1963 A

Report AEM-H1-28

(12)

AD A115101

STRUCTURAL INELASTICITY XXVIII

Final Report on Structural Inelasticity
at the University of Minnesota

Contract N00014-75-C-0177

Philip G. Hodge, Jr., Professor of Mechanics

Patrick Tait, Research Assistant

James Malone, Research Assistant

Department of Aerospace Engineering and Mechanics
University of Minnesota
Minneapolis, Minnesota 55455

March, 1982

Technical Report

Qualified requesters may obtain copies of this report from DDC

Prepared for

OFFICE OF NAVAL RESEARCH
Arlington, VA 22217

OFFICE OF NAVAL RESEARCH
Chicago Branch Office
536 South Clark St.
Chicago, IL 60605

DTIC FILE COPY

DTIC
ELECTE
JUN 0 4 1982
S D
E

This document has been approved for public release and sale; its distribution is unlimited.

82 04 27 109

SECURITY CLASSIFICATION OF THIS PAGE (When Data Entered)

REPORT DOCUMENTATION PAGE

READ INSTRUCTIONS BEFORE COMPLETING FORM

1. REPORT NUMBER
AEM-H1-28

2. GOVT ACCESSION NO.
AD-A115 107

3. RECIPIENT'S CATALOG NUMBER

4. TITLE (and Subtitle)
STRUCTURAL INELASTICITY XXVIII

5. TYPE OF REPORT & PERIOD COVERED
Technical Report

6. PERFORMING ORG. REPORT NUMBER

7. AUTHOR(s)
Philip G. Hodge, Jr., Prof. of Mechanics

8. CONTRACT OR GRANT NUMBER(s)
N00014-75-C-0177

9. PERFORMING ORGANIZATION NAME AND ADDRESS
University of Minnesota
Minneapolis, Minnesota 55455

10. PROGRAM ELEMENT, PROJECT, TASK AREA & WORK UNIT NUMBERS
NR 064-429

11. CONTROLLING OFFICE NAME AND ADDRESS
OFFICE OF NAVAL RESEARCH
Arlington, VA 22217

12. REPORT DATE
March 1982

13. NUMBER OF PAGES
136

14. MONITORING AGENCY NAME & ADDRESS(if different from Controlling Office)
OFFICE OF NAVAL RESEARCH
Chicago Branch Office
536 South Clark St.
Chicago, IL 60605

15. SECURITY CLASS. (of this report)
Unclassified

15a. DECLASSIFICATION/DOWNGRADING SCHEDULE

16. DISTRIBUTION STATEMENT (of this Report)

This document has been approved for public release and sale; its distribution is unlimited.

~~Qualified requestors may obtain copies of this report from DDC~~

17. DISTRIBUTION STATEMENT (of the abstract entered in Block 20, if different from Report)

18. SUPPLEMENTARY NOTES

19. KEY WORDS (Continue on reverse side if necessary and identify by block number)
Plasticity, quadratic programming, shakedown

20. ABSTRACT (Continue on reverse side if necessary and identify by block number)

A summary and bibliography are presented of the investigations of structural inelasticity which were carried out at the University of Minnesota under the sponsorship of the Office of Naval Research during the period 1971-1981. Also included are preliminary reports on two investigations still in progress.

DD FORM 1 JAN 73 1473 EDITION OF 1 NOV 65 IS OBSOLETE
S/N 0102-014-6601

SECURITY CLASSIFICATION OF THIS PAGE (When Data Entered)

Contract N14-67-113-25 AEM Report H1-28

Project NR 064-429 University of Minnesota

FINAL REPORT ON INVESTIGATIONS OF STRUCTURAL INELASTICITY AT THE UNIVERSITY OF MINNESOTA[1]

by

Philip G. Hodge, Jr.[2]

Patrick Tait[3]

James Malone[3]

ABSTRACT

A summary and bibliography are presented of the investigations of structural inelasticity which were carried out at the University of Minnesota under the sponsorship of the Office of Naval Research during the period 1971-1981. Also included are preliminary reports on two investigations still in progress.

---

[1]Reproduction in whole or in part is permitted for any purspose of the United States Government. Distribution of this document is unlimited.

[2]Professor of Mechanics, University of Minnesota.

[3]Research Assistants, University of Minnesota.

FINAL REPORT ON STRUCTURAL INELASTICITY AT THE UNIVERSITY OF MINNESOTA

by Philip G. Hodge, Jr.

1. INTRODUCTION

Contract ONR N14-67-A-113-25, Project No. NR 064-429 was in operation between the Office of Naval Research and the University of Minnesota from September 1, 1971 through August 31, 1974. It was succeeded by Contract N14-75-C-0177 which began September 1, 1974 and terminated December 15, 1981. Both contracts have been under the direction of Dr. P. G. Hodge, Jr., Professor of Mechanics. Also working on the contracts have been Professor R. Foral and J. Skrzypek, Drs. I. Berman, M. Dusek, V. K. Garg, H. v. Rij, and P. K. Sinha, and Messrs. G. Hanson, D. Korpella, J. Malone, K. Sadhal, P. Tait, D. White, R. Wozniak, and Ma Zeen.

The purpose of the two contracts has been investigations in "Structural Inelasticity." Results were written up as they were obtained and were issued as technical reports and/or as publications in journals or symposia volumes. In order to avoid undue duplication, this "Final Report" has been divided into three main parts.

Section 2 consists of the title and abstract of the twenty seven technical reports issued under the contract, together with their publication data. Copies and/or reprints of the complete

reports are available on request.

The remaining two sections contain preliminary reports on two investigations which were still in progress at the termination of the current contract. Specifically, Sec. 3 reports on the development of a quadratic-programming routine for solving elastic-plastic grid problems, and Sec. 4 contains some preliminary results concerning shakedown under distributed loads.

A new contract N14-82-K-20 has been awarded to the University of Minnesota by the Office of Naval Research. It is anticipated that investigations in Secs. 3 and 4 will be completed and technical reports on them issued under this new contract.

2. SUMMARY OF TECHNICAL REPORTS

2.1 Report AEM-H1-1.

"Plastic Design of a Storage Tank"
by Philip G. Hodge, Jr.
Proc. Int. Symp. Plastic Analysis of Structures, A. Negoita, ed., Jassy, Romania, 1972, Vol. 1. pp. 346-374.

A cylindrical tank of radius A, uniform thickness H, and height L rests on level ground on one end, and is filled with a liquid of density ρ. It is desired to design it to have a specified safety factor against plastic collapse. The solution over the entire range of shell sizes is expressed by simple parametric expressions for the dimensionless geometrical ratio $\gamma = 2L^2/AH$ and the dimensionless density $\alpha = (2\rho g L^3)/(3\sigma_0 H^2)$ where σ_0 is the yield stress. Curves are obtained such that given any four of the quantities H, A, L, σ_0, ρ, the fifth can easily be found. It is noted that if the tank is perfectly tight and is completely filled with an incompressible liquid, then it will be substantially stronger due to the constraint of maintaining a constant volume during deformation.

2.2 Report AEM H1-2

"A Consistent Theory for the Elastic-Plastic Stability of an Annular Plate Under Inner Tension,"
by Ralph F. Foral and Philip G. Hodge, Jr.

An annular plate is subjected to an in-plane tensile loading at its inner edge. The plate is made of an elastic/plastic material which satisfies the Tresca yield criterion with linear isotropic hardening. The buckling load at which an out-of-plane deformation first becomes possible is found for a wide range of plate and hardening parameters. Depending upon the values of these parameters, buckling may occur in the elastic, elastic-plastic, or fully plastic stage of the in-plane deformation.

2.3 Report AEM H1-3

"Computer Solutions of Plasticity Problems"
by Philip G. Hodge, Jr.
"Problems of Plasticity"
by A. Sawczuk
ed. (Proc. Int. Symp. on Foundations of Plasticity, Warsaw, 1972), Noordhoff Int. Publ., Leyden, 1974, pp. 261-286.

In recent years, finite-element methods have proved to be a very useful tool in obtaining solutions to problems of practical importance for both elastic and inelastic structures. Because the need for solutions is so great, and because the results predicted by finite-element solutions are reasonable, primary interest has been in the establishment of efficient computer programs for the solution of large-scale problems. As a result, some theoretical considerations which may be important in extended applications of the methods have tended to be overlooked. The present paper reviews the current state of the art, focuses on some of these questions and recent work that has been done towards obtaining answers, and suggests some desirable directions for future research.

Accession For
NTIS GRA&I ☒
DTIC TAB ☐
Unannounced ☐
Justification
By
Distribution/
Availability Codes
Avail and/or
Dist Special
A

DTIC COPY INSPECTED 2

2.4 Report AEM H1-4

"Complete Solutions for Elastic-Plastic Trusses"
by Philip G. Hodge, Jr.
SIAM J. Appl. Math. 25, 435-447 (1973)

The complete solutions for stresses and displacements of an elastic truss may either be found by direct solution of the defining equations or by using either of the elastic minimum principles. From both a theoretical and computational approach, the three methods are very similar.

Three related methods are available for elastic/perfectly-plastic trusses, but here they are quite distinct. It is shown that none of the three is entirely satisfactory, but that a combined method leads directly to a complete solution. In the proposed method, the static minimum principle is first used to find the stress rates and stresses, and some information from the stress solution is fed into the kinematic minimum principle to obtain the velocities and displacements.

2.5 Report AEM H1-5

"Some Applications of the Principle of Virtual Work"
by Philip G. Hodge, Jr.
Proc. 4th Canadian Cong. Appl. Mech., A. Biron, ed., Montreal, 1973 pp. G-37-50.

The Principle of Virtual Work is reviewed in its relation to continuum mechanics. A formal three-dimensional proof is given for reference, and the principle is also stated in terms of generalized variables. Applications are given for general theorems such as uniqueness for specific media, for derivation of structural theories independently of material characteristics, and to numerical methods of finite element analysis.

2.6 Report AEM H1-6

"A Finite Element Method for Plasticity Problems"
by Philip G. Hodge, Jr., Vijay K. Garg, and Subhash C. Anand
"Developments in Theoretical and Applied Mechanics VII"
(Proc. 7th SECTAM), S. J. Heller, ed., Catholic Univ.,
Washington D.C., 1974, pp. 364-383.

A method is presented for finding complete solutions (stresses and displacements) for plasticity problems. The problem is first approximated by a finite-element model and a rate formulation is used. An exact solution for the stress rates is obtained by solving the quadratic programming problem which expresses the static minimum principle. Using some but not all of the information from this solution, the velocities are easily obtained from the kinematic minimum principle.

The method is applied to a model for a wheel rolling on a rigid track. Maximum elastic loads, collapse loads, and shakedown loads are found for both gravity and hub loading. For loads between shakedown and collapse it is found that failure is incremental for gravity loading but cyclic for hub loading.

2.7 Report AEM H1-7

"Elastic-Plastic Analysis of a Wheel Rolling on a Rigid Track"
by V.K. Garg, Subhash C. Anand, and Philip G. Hodge, Jr.,
Int. J. Solids Structs. 10, 945-956 (1974).

A consistent finite element model for a circular wheel is developed based on triangular and quasi-triangular domains and a piecewise linear displacement field. The minimum stress-rate principle of plasticity is used to obtain solutions of two-dimensional continuum problems with internal unloading. A piecewise approximation of the Tresca yield condition is used. Elastic-plastic solutions of a wheel rolling on a rigid track under its own weight and a hub load are obtained for the first few revolutions until a steady state condition is reached. Shake-down conditions for the wheel are demonstrated.

2.8 Report AEM H1-8

"Post-Yield Behavior of a Beam with Partial End Fixity"
by Philip G. Hodge, Jr.
Int. J. Mech. Sci. 16, 385-388 (1974).

A simply supported beam can undergo a relative axial displacement proportional to the induced axial force. Complete formulas and curves are obtained for transverse displacements of the order of the beam thickness.

2.9 Report AEM H1-9

"Finite Element Methods in Plasticity"
by Philip G. Hodge, Jr.
Proc. 7th U.S. Nat. Congr. Appl. Mech., S.K. Datta, ed.
(Boulder, 1974), ASME, 1974, pp. 114-119

When finite element methods are applied to elastic problems, the essential kinematic variables are usually taken to be as continuous as possible. It is shown here that the restriction that beam slopes be continuous is not necessary. Four different models are considered, and it is demonstrated that for a given number of degrees of freedom, models which allow discontinuous slopes give better results in the plastic range.

2.10 Report AEM H1-10

"A New Model for Elastic-Plastic Trusses"
by Kuldip S. Sadhal and Philip G. Hodge, Jr.

The phenomenon of upper yield and lower yield for steel bars under uniaxial stress is well known but not fully understood. The actual behavior of a bar at stress levels between the two yield stresses will depend upon many minor variables which may not be controlled or even known, so that from a pragmatic point of view it is indeterminate. Several models are proposed in which the behavior of a bar in the indeterminate range is chosen for computational convenience. The models are applied to several examples, and their advantages and disadvantages are discussed. It is concluded that the specific models described are not reasonable tools for practical engineering problems, but that the concept is worthy of further study.

2.11 Report AEM H1-11

"A Review of Some Piecewise Linear Theories of Plastic Strainhardening"
by Philip G. Hodge, Jr. and Irwin Berman
"Constitutive Equations in Viscoplasticity: Computational and Engineering Aspects"
J.A. Stricklin and K.J. Saczalski
eds. AMD-20, ASME, 1976.

A review is presented of work on piecewise linear plasticity done by the senior author and his students from 1955 to 1959. A theory for an anisotropic material with 9 material constants is presented and some experiments suggested for determining the constants. Various classical theories may be obtained as special cases.

2.12 Report AEM H1-12

"Large Rotationally-Symmetric Plastic Deformations of a Sandwich-Toroidal Shell"
by Jacek Skrzypek and Philip G. Hodge, Jr.

A nonlinear theory of large rotationally-symmetric plastic deformation of a sandwich-toroidal shell has been formulated. The generating curve for the toroid is assumed to be open and of an arbitrary shape. Deformation of the shell, described by the linear Cauchy's measure, is governed by the Love-Kirchoff hypothesis. On the basis of the principle of virtual work non-linear equations of equilibrium have been derived. The material of the sandwich sheets is assumed to be rigid/perfectly-plastic and to obey the Levy-Mises theory of plastic flow and Huber-Mises-Hencky yield condition.

The fundamental equations have been reduced to a system of six, coupled, ordinary, nonlinear differential equations which are, however, linear with respect to the first derivatives of unknown functions. By the use of a numerical procedure the initial/boundary problem can be reduced to a boundary value problem only, for each step of the loading process. Different types of boundary problems as well as continuity requirements have been discussed.

2.13 Report AEM H1-13

"Finite Element Models for Elastic-Plastic Structures"
by Philip G. Hodge, Jr.
"Developments in Theoretical and Applied Mechanics 8,
R.P. McNitt, ed., VPI, SU Press, 1976.

It is shown how a consistent finite element model for an elastic-plastic material can be derived by a well-defined sequence of elementary steps. A restricted kinematically admissible field is defined in each generic element and substituted into the internal and external work to lead naturally to appropriate definitions for generalized stresses, strains and forces. The Principle of Virtual Work then leads to the necessary static relations between the generalized stresses. Finally, elastic-plastic constitutive relations are derived from the expression for internal work and some simplifications are suggested. The theory is illustrated with finite element models for beams, plane strain, plain stress, and torsion.

2.14 Report on AEM H1-14

"Automatic Piecewise Linearization in Ideal Plasticity"
by Philip G. Hodge, Jr.
Comp. Meth. in Appl. Mech. & Eng. 10, 249-272 (1977)

A method is proposed for constructing a piecewise linear approximation to an arbitrary yield function. The approximation is constructed in the course of solving a given boundary-value problem. Its use is illustrated with some simple examples.

2.15 Report AEM H1-15

"Limit Analysis and Coublomb Friction"
by Philip G. Hodge, Jr.

The theorems of limit analysis are not valid if part of the boundary is pressed against a rigid surface and constrained by coulomb friction. In reference to a problem of inverted extrusion, we show how conventional limit analysis can be extended to obtain upper and lower bounds on the force necessary for extrusion.

2.16 Report AEM H1-16

"Elastic-Plastic Plate with Arbitrary Poisson's Ratio"
by Philip G. Hodge, Jr.
J. Appl. Mech. 45, 205-206, (1978).

An earlier solution for the bending of a built-in circular plate made of an incompressible elastic/perfectly-plastic material is extended to include any value of Poisson's ratio ν. Qualitative differences in the nature of the solution are observed for $0 \leq \nu < 1/5$, $1/5 < \nu < 1/3$, and $1/3 < \nu \leq 1/2$.

2.17 Report AEM H1-17

"Theory of Plastic Structures"
by Philip G. Hodge, Jr.
"Structural Engineering and Structural Mechanics",
K.S. Pister, Ed., Prentice-Hall, Englewood Cliffs, NJ,
1980, pp. 57-91.

A sampling is given of the applications of plasticity theory to structures. Relations between various theories which include or neglect strain hardening and elastic strains are discussed. Applications are given to trusses, beams, frames and circular plates. The paper concludes with some general observations on the use of plasticity theories with finite-element models.

2.18 Report AEM H1-18

"A Slip Model for Finite Element Plasticity"
by Hendrik van Rij and Philip G. Hodge, Jr.
J. Appl. Mech. 45, 205-206 (1978).

Conventional finite-element models are based on displacement or velocity fields which are at least continuous. However, it is known that perfectly plastic materials may exhibit discontinuities of the tangential velocity component along certain lines. In this investigation a two-dimensional finite element model is proposed which will allow for such discontinuities.

A regular pattern of triangular elements is assumed. The elements are assumed to be rigid, and across the line separating any two adjoining elements the normal displacement component is continuous, but a discontinuity may exist in the tangential component. The defining equations - compatibility, equilibrium, and constitutive - are developed with the aid of the Principle of Virtual Work.

Prandtl's punch problem is solved under plane strain conditions. Comparison is made with existing analytical and other numerical solutions, in order to evaluate the merits of allowing for discontinuities.

2.19 Report AEM H-19

"Review of Moisture Diffusion in Composites"
by P.K. Sinha

The effect of moisture diffusion in composite materials is reviewed. Pertinent equations are listed and various special solutions are given. Extensive references are quoted. Several suggestions are made for future research in the area.

2.20 Report AEM H1-20

"Failure of Composites"
by P.K. Sinha

A review of composites materials is presented. Primary emphasis is on fiber-reinforced composites. Particular attention is paid to various failure mechanisms in tension, compression, and shear. Existing results are summarized and suggestions are given for future research.

2.21 Report AEM H1-21

"Finite Element Models with Velocity Discontinuities"
by Hendrik M. van Rij and Philip G. Hodge, Jr.
J. Appl. Mech. 45, 527-532 (1978).

Conventional finite-element models are based on displacement or velocity fields which are at least continuous. However, it is known that perfectly plastic materials may involve discontinuities of the tangential velocity component along certain lines. In this investigation, two two-dimensional finite element models are proposed which will allow for such discontinuities.

A regular pattern of triangular elements is assumed. In the first model, the elements are assumed to be rigid, and in the second model, we have a linear displacement field in each element. Across the line separating any two adjoining elements the normal displacement component is continuous, but a discontinuity may exist in the tangential component. The defining equations-compatibility, equilibrium, and constitutive - are developed with the aid of the Principle of Virtual Work.

Prandtl's punch problem and tension in notched bars are solved under plane strain conditions. Comparison is made with existing analytical and other numerical solutions, in order to evaluate the merits of allowing for discontinuities.

2.22 Report AEM H1-22

"A Finite-Element Model for Plane-Strain Plasticity"
by Philip G. Hodge, Jr. and Hendrik M. Van Rij
J. Appl. Mech. 46, 536-542 (1979).

A finite-element model is proposed which allows for both straining within each element and slip between two elements. Basic equations are derived and are shown to almost completely uncouple into two constituent components: the conventional finite-element equations for continuous displacement fields and the "slip" equations which were recently derived for a model based on slipping of rigid triangles. The model is applied to the Prandtl punch problem and is shown to combine the best features of its two constituents.

2.23 Report AEM H1-23

"A piecewise linear theory of plasticity for an initially isotropic material in plane stress"
by Philip G. Hodge, Jr.
Int. J. Mech. Sci. 22, 21-32 (1980).

A 20-faced polyhedron is chosen as a reasonable piecewise linear approximation to either the Mises or Tresca yield criterion. Strain hardening and motion of the faces during hardening are assumed to be linear functions. Subject to the above assumptions, to initial isotropy, and to some reasonable symmetry requirements it is shown that the most general possible theory contains 11 material constants. Some simple experiments with a thin-walled tube are suggested for determining these constants.

2.24 Report AEM H1-24

"Examples of non-uniqueness in contained plastic deformation"
by Philip G. Hodge, Jr. and David L. White
J. Appl. Mech. 47, 223-227 (1980).

It is well known that in a well-defined boundary-value problem for an elastic/perfectly-plastic structure the displacements are unique if the structure is everywhere elastic, and they are not unique at the yield-point load. The present paper is concerned with the range of contained plastic deformation between these two extremes. Several examples are given in which more than one displacement field exists for loads less than the yield-point load. The significance of this phenomenon is commented on from a physical, mathematical, and computational point of view.

2.25 Report AEM H1-25

"Computation of Non-Unique Solutions of Elastic-Plastic Trusses"
by David L. White and Philip G. Hodge, Jr.
Comp. and Struct. 12, 769-774 (1980).

It has recently been shown that the solution to certain well-defined boundary value problems for elastic/perfectly-plastic structures is non-unique. The present paper is concerned with the ability of finite-element computer programs to handle such solutions. Some problems arising from non-uniqueness are documented and techniques for circumventing those problems are evaluated by exploring the response of the program NonSAP to a variety of trusses with non-unique solutions.

2.26 Report AEM H1-26

BEAMPLOT: A program for finding the yield-point load of transversely loaded rectangular grids
by Patrick Tait and Philip G. Hodge, Jr.

An interactive computer program for finding the yield-point load of a transversely loaded rectangular grid is described. The maximum statically-admissible multiplier and an associated moment distribution are found by Linear Programming.

2.27 Report AEM H1-27

Computer Methods in Plastic Structural Analysis
Philip G. Hodge and James Malone
(Appears as a new Chapter 14 in the revised edition of "Plastic Analysis of Structures" by Philip G. Hodge, Jr., R.E. Krieger Publ. Co., Inc., Malabar, FL., 1981).

A tutorial review is presented of some of the computer methods useful in the plastic analysis of structures. Each method is illustrated with a trivially simple problem which can be solved without a computer and by one or more larger problems solved with the aid of a computer. The methods described include direct elastic-plastic analysis, linear programming, gradient and simplex methods for unconstrained minimization, the SUMT method for constrained minimization, and use of finite-element methods for plate problems. Applications are made to trusses, frames, grids, arches, and plates.

3. BEQUAD

BEQUAD is a quadratic-programming routine for the elastic-plastic solution of transversely loaded rectangular grids.

1. Introduction. BEQUAD is a FORTRAN computer program for finding the "time" history of transversely loaded structural grids. A grid consists of two sets of parallel beams at right angles to each other, as shown in Fig. 1; a given set of transverse loads $f_{i,j}$ (some of which may be zero) is applied to the nodes where two beams intersect. One objective is to find the maximum safety factor P of the grid, defined as that multiplier of the given loads such that the grid will just collapse under the loads $Pf_{i,j}$, but will support any smaller multiplier of the loads. An example of such a structure is found in many buildings where a floor is supported by a grid structure.

In the analysis of the problem, we will assume the grid is made of an elastic perfectly-plastic material, and deformations are small, prior to collapse. We shall also neglect any torsional strength in the beams. The beams will have a maximum bending moment which can be transmitted across a beam section.

Under these assumptions an appropriate minimum principle may be formulated such that its solution, subject to a statically admissible distribution of beam moments, yields a means of finding the "time" history of structural grids. The moments must be everywhere in equilibrium with the loads $Pf_{i,j}$, and nowhere exceed the maximum bending moment (yield moment) of the beam.

BEQUAD solves the problem by expressing it as a Quadratic Programming problem and using previously prepared subroutines from

the Harwell Subroutine Library to solve it. Sections 5 and 6 of this guide describe the program from the user's point of view. First, however, in Sec. 2 we will formulate and describe the "rate" principle needed to solve our grid problem, and in Sec. 3 the equilibrium equations are derived. Section 4 will show that the grid problem can be converted into one of Quadratic Programming. Finally, Sec. 7 will give the results of some typical problems.

2. Rate Principle. We are concerned here with a transversely loaded grid as the loads are slowly increased in a fixed but arbitrary proportion. Let f_α denote a fixed set of transverse loads on the joints α, and consider the response of the grid under the loads $p(t)f_\alpha$ as p is slowly increased.

At a generic time t_o assume that all quantities have known values, and we wish to determine their rates. Let $\dot{M}^*(x)$ denote any set of moment rates which are in equilibrium internally and with the external load rates $\dot{p}^* f_\alpha$, and which also satisfy the plasticity constraints:

$$\text{If } M = Y \text{ then } \dot{M}^* \leq 0 \tag{1a}$$

$$\text{If } M = -Y \text{ Then } \dot{M}^* \geq 0 \tag{1b}$$

where Y is the yield moment. Further, let $\dot{K}^*(x)$ be curvature rates given by

$$\dot{K}^* = \dot{M}^*/EI \tag{2}$$

where E is Young's modulus and I the transverse moment of inertia. Then, as we shall show, the quantity

$$A_c^* \equiv \Sigma_k \tfrac{1}{2}\int_0^{L_k} \dot{M}^* \dot{K}^* \, dx - \dot{p}^* \Sigma_\alpha f_\alpha v_\alpha \tag{3}$$

is a minimum for the actual elastic-plastic rate solution $\dot{M}$, $\dot{p}$, $\dot{K}$.

To prove this result, which is essentially Greenberg's principle [1]* (see [2] for a text account), we must show that the quantity.

$$\Delta A_c \equiv A_c^* - A_c$$

$$= \tfrac{1}{2} \Sigma_k \int_0^{L_k} (\dot{M}^* \dot{K}^* - \dot{M} \dot{K}) - (\dot{p}^* - \dot{p}) \Sigma_\alpha f_\alpha v_\alpha \tag{4}$$

is non-negative. Now, by analogy to the principle of virtual work,

$$(\dot{p}^* - \dot{p}) \Sigma_\alpha f_\alpha v_\alpha = \Sigma_k \int_0^{L_k} (\dot{M}^* - \dot{M}) \dot{K} \, dx \tag{5}$$

hence we can write (4) in the form

$$\Delta A_c = \tfrac{1}{2} \Sigma_k \int_0^{L_k} W(x) \, dx \tag{6a}$$

where

$$W(x) = \dot{M}^* \dot{K}^* - 2\dot{M}^* \dot{K} + \dot{M} \dot{K} \tag{6b}$$

For the actual solution the curvature rate must satisfy the elastic-plastic flow law

$$\dot{K} = \dot{M}/EI + \dot{K}^p \tag{7a}$$

$$\text{IF } |M| < Y \text{ or } M\dot{M} < 0 \text{ then } \dot{K}^p = 0 \tag{7b}$$

$$\text{ELSE } M\dot{K}^p \geq 0 \tag{7c}$$

*References are listed on page 46.

Using (7a) and (2) we can write (6b) as

$$W = (1/EI)(M^* - \dot{M})^2 + W_p \tag{8}$$

where

$$W_p = \dot{M} \dot{K}^p - 2\dot{M}^* \dot{K}^p \tag{9}$$

Now, in view of (7b), $\dot{K}^p = 0$ unless $M = \pm Y$ and $\dot{M} = 0$. Therefore, in every case $\dot{M}\dot{K}_p = 0$ and

$$W_p = -2 \dot{M}^* \dot{K}^p \tag{10}$$

where $W_p = 0$ unless $M = \pm Y$. But if $M = Y$ then it follows from (1a) and (7c) that

$$\dot{M}^* \leq 0 \text{ and } \dot{K}^p \geq 0 \tag{11a}$$

whereas if $M = -Y$,

$$\dot{M}^* \geq 0 \text{ and } \dot{K}^p \leq 0 \tag{11b}$$

Therefore, in every case $W_p \geq 0$ from which it follows from (8) that $W \geq 0$ and hence from (6a) that

$$\Delta A_c \geq 0, \quad \text{QED} \tag{12}$$

Finally, we note that the time scale in Eqs. (1) and (7) is completely arbitrary. Therefore, we may arbitrarily choose it so that

$$\Sigma_\alpha f_\alpha v_\alpha = 1 \tag{13}$$

Further, we assume that each beam segment k in the grid has constant modulus E_k and moment of inertia I_k. Finally we incorporate (2)

in (3) and drop the superscripts to write the minimum principle as follows:

> Among all moment rates which satisfy Eqs. (1) and are in equilibrium internally and with the joint loads pf_α, the actual solution to the elastic-plastic problem will minimize

$$\Lambda_c = \tfrac{1}{2}\,\Sigma_k (1/E_k I_k)\int_0^{L_k} \dot{M}_k^{\,2}\,dx - \dot{p} \tag{14}$$

To find the form of $\int \dot{M}^2(x)dx$ we will consider a general horizontal beam segment k (a segment away from the boundaries) with bending rate moments $\dot{M}_{i,j}$ on the left end and $\dot{M}_{i,j+1}$ on the right end, as in figure 2. If the (rate) moment varies linearly across the segment, we have

$$\dot{M}(x) = \dot{M}_{i,j}(L_k - x) + \dot{M}_{i,j+1}\cdot x/L_k \tag{15}$$

hence

$$\int_0^{L_k} \dot{M}^2(x)dx = (L_k/3)(\dot{M}^2_{i,j} + \dot{M}_{i,j}\cdot\dot{M}'_{i,j+1} + \dot{M}^2_{i,j+1}) \tag{16a}$$

Similarly, for a vertical beam with (rate) moment $M'_{i,j}$ at the top end and $M'_{i+1,j}$ at the bottom end we have

$$\int_0^{L'_k} \dot{M}'^2(x)\,dx = \frac{L'_k}{3}\,(\dot{M}'_{i,j} + \dot{M}'_{i,j}\cdot\dot{M}'_{i+1,j} + \dot{M}'^2_{i+1,j}) \tag{16b}$$

Substitution of (16a) and (16b) into equation (14) gives the general form

$$\Lambda_c = \frac{1}{2EI_{zz}}\sum_\alpha \frac{L_\alpha}{3}\,(\dot{M}^2_{i+j} + \dot{M}_{i,j}\cdot\dot{M}_{i,j+1} + \dot{M}^2_{i,j+1}$$
$$+ \frac{1}{2E'I'_{zz}}\sum_\beta \frac{L'_\beta}{3}\,(\dot{M}'^2_{i,j} + \dot{M}'_{i,j}\cdot\dot{M}'_{i+1,j} + \dot{M}'^2_{i+1,j}) - \dot{P} \tag{17}$$

where Σ implies a sum on each of the beam segments; α is the number of horizontal beam segments, and β is the number of vertical beam segments. Equation (2.6) in Appendix A shows this equation written out for a specific problem.

Beam segments next to boundaries have a slightly different form depending onthe type of boundary condition. We will consider four possible boundary conditions along each side, plus the possibility of corner supports. The four possibilities are (a) free cantilever, (b) free cross beam, (c) simply supported, (d) clamped. Figure (3) illustrates grids with various combinations of edge type. Unless the beam is clamped, the (rate) moment at its end must be zero. Therefore, if the left side of the beam is case (a), (b), or (c); $\dot{M}_{i,1} = 0$ for all i. Thus for the sum of horizontal beam segments next to the left edge the first two (rate) moment terms in Eq. (17) are replaced by zero. A similar remark applies to segments next to the right, top, or bottom boundaries if the boundary condition there is anything other than clamped. Note that if an edge is clamped, the (rate) moment is unknown and Eq. (17) is unchanged for segments along the edge.

3. <u>Equilibrium Equation</u>. As stated in the previous section, we are looking for a solution which minimizes Eq. (17) and satisfies internal equilibrium. That is we wish to minimize Eq. (17) subject to equilibrium requirements.

We consider, first, a generic interior node ij and derive an equilibrium equation. Fig. 4 shows a free body diagram and defines the lengths and sign conventions. Each of the four beam segments at the

node has shear forces and (rate) moments acting on it. Since torsional moments are neglected, the two horizontal (rate) moments $\dot{M}_{i,j}$ at node i,j must be equal, as must the vertical (rate) moments $\dot{M}'_{i,j}$. Out-of-plane and moment equilibrium of the beam segment L_{j-1} require

$$\dot{V}_1 = \dot{V}_2 = (\dot{M}_{i,j} - \dot{M}_{i,j-1})/L_{j-1} \tag{18}$$

with similar expressions for each of the other segments.

Satisfying shear force equilibrium at the node, we have from Fig. 4,

$$\dot{V}_2 + \dot{V}_3 + \dot{V}_6 + \dot{V}_7 = \dot{p}f_{i,j} \tag{19}$$

where $\dot{p}$ is the rate load factor and $f_{i,j}$ is the load applied at the location i,j. Substituting the (rate) moment relations such as (18) in the shear equation gives

$$\frac{\dot{M}_{i,j} - \dot{M}_{i,j-1}}{L_{j-1}} + \frac{\dot{M}_{i,j} - \dot{M}_{i,j+1}}{L_j} + \frac{\dot{M}'_{i,j} - \dot{M}'_{i-1,j}}{L'_{i-1}} +$$

$$\frac{\dot{M}_{i,j} - \dot{M}'_{i+1,j}}{L'_i} - \dot{p}f_{i,j} = 0 \tag{20}$$

This equation holds for all nodes except near or on boundaries.

For nodes next to or on a boundary the procedure is the same, but the boundary condition defines some of the moments so that Eq. (20) will become simplified.

Again, referring to figure 4, if the left side of the beam is case (a), (b), or (c); $\dot{M}_{i,1} = 0$ for all i. Thus for j=2, one of the (rate) moments in Eq. (20) is replaced by zero. A similar remark applies to j=m-1, i=2, or i=n-1 when the right, top, or

bottom edge, respectively, is anything other than clamped. However, if an edge is clamped, the (rate) moment is unknown and Eq. (20) for the neighboring column or row is unchanged.

For nodes on the boundary the changes are more significant. If the left edge is a free cantilever, then there are no vertical beams and, of course, there is no beam segment to the left of the node. Thus Fig. 4 reduces to Fig. 5a, and Eq. (20) reduces to

$$-\dot{M}_{i,2}/L_1 - \dot{p}f_{i,1} = 0 \tag{21a}$$

with similar simple equations if other edges are free cantilever.

On the other hand, if there is a free cross beam along the left edge, there will be three beam segments as shown in Fig. 5b, and Eq. (20) takes the form

$$\frac{-\dot{M}_{i,2}}{L_1} + \frac{\dot{M}'_{i,1} - \dot{M}'_{i-1,1}}{L'_{i-1}} + \frac{\dot{M}'_{i,1} - \dot{M}'_{i+1,1}}{L'_i} = \dot{p}f_{i,1} \tag{21b}$$

Again, there are similar simplifications for the other edges.

If the end of a beam is clamped or simply supported, then vertical motion is prohibited and the support provides an external reaction force $\dot{R}_{i,j}$. It follows that vertical equilibrium at such a node serves only to define $\dot{R}_{i,j}$, and does not constitute a constraint on the moments. For our purposes, then, we do not enforce Eq. (20) on edges of type (c) or (d).

Since each edge may independently be of any of the four types, there would appear to be many different possibilities at the corners. However, if either edge at a corner is of type (c) or (d) (corners C, D, E, or H in Fig. 4) there will be no Eq.(20), and if both edges are type (a) (corner A) there are no beams at

the corner, hence the load must be zero. If the top edge is a free cross beam and the left edge a free cantilever, (corner B) the upper left corner node is governed by Eq.(21a) with i=1. Other corners of this type have similar equations.

Finally, if both the top and left edge are cross beams, we allow for two possibilities. If they are both free cross beams (corner G in Fig. 3), as shown in Fig. 5c, Eq. 21b simplifies further to

$$-\dot{M}_{1,2}/L_1 - \dot{M}'_{2,1}/L'_1 - \dot{P}f_{1,1} = 0 \qquad (21c)$$

with similar equations at other corners. The other possibility is that although the cross beams are otherwise free, the corner rests on a simple support as at F in Fig. 3. In this case, of course, Eq. (20) is not applicable.

Other modifications can be made in Eq. (20) and Eq. (8) if the node is on a line of symmetry. Such lines may be vertical or horizontal, may be along a beam or between two beams, or may be a diagonal of the grid. We shall not detail the resulting forms of Eq. (20) or (17), but we note that vertical and/or horizontal lines of symmetry are incorporated in BEQUAD and their use will be described in Sec. 5.

For any symmetric beam section the yield moment may be regarded as a known property of the material yield stress σ_0 and dimensions of the beam cross section. It corresponds to the top and bottom halves of the section being at the uniform stresses $-\sigma_0$ and $+\sigma_0$, respectively. For example, the yield moments for the rectangular and T sections (neglecting fillets) shown in Fig. 6 are, respectively,

$$M_0 = \sigma_0 wh^2/-4 \qquad (22a)$$

$$M_0 = \sigma_0[t_w(h/2 - t_f)^2 - wt_f(h - t_f)] \qquad (22b)$$

We assume that all horizontal beams have the same yield moment M_0 and all vertical yield moments are M'_0. Then the moments must satisfy Eqs. (1), i.e.

$$-M_0 \le M_{i,j} \le M_0 \qquad (23a)$$

$$-M'_0 \le M'_{i,j} \le M'_0 \qquad (23b)$$

Suppose we found rate moments which minimize Eq. (17) and satisfy Eq. (20), i.e. $\dot{M}_{i,j}$, $\dot{M}'_{i,j}$, and $\dot{P}$ are known. Then the moments $M_{i,j}$, $M'_{i,j}$, and load factor P can be found as linear functions of "time" (t) by integrating the solution. We now look for the largest "time" such that Eq. (23) is still satisfied, i.e. we increase the load linearly until a grid member reaches yield. If, at this "time" the collapse load has not been reached we look for a new solution with the further restriction that all moments which are at yield must have their "rate" counter-parts satisfy

$$|\dot{M}_{i,j}| \le 0 \qquad (24a)$$

$$|\dot{M}'_{i,j}| \le 0 \qquad (24b)$$

That is a moment must not increase in magnitude if it was at its yield point the previous "time".

A complete "time" history of the grid can be found by continuing this process until the grid reaches collapse. An example of this process is shown in Appendix B.

4. Quadratic Programming. Solving the minimization problem requires the use of Quadratic Programming. A typical Quadratic Programming problem is concerned with a vector $\underline{x}$, a scalar objective function

$$f(\underline{x}) = \tfrac{1}{2}\, \underline{x}^T \underline{\underline{A}}\, \underline{x} - \underline{b}^T \underline{x} \tag{25a}$$

and constraints

$$\underline{\ell} \le \underline{x} \le \underline{u} \tag{25b}$$

$$\underline{d} \le \underline{\underline{C}}^T \underline{x} \tag{25c}$$

where $\underline{\underline{A}}$ is symmetric and where any of the inequalities may be designated as strict equalities. The Quadratic Programming problem may then be stated as

Find a vector $\underline{x}$ which
minimizes $f(\underline{x})$ subject to (25b) and (25c).

The Quadratic Programming problem and our grid problem are almost identical. We can interpret each $\dot{M}_{i,j}$, $\dot{M}_{i,j}$, and $\dot{P}$ as components of a vector $\underline{x}$; and form the matrix $\underline{\underline{A}}$ from the coefficients of the quadratic part of Eq. (17) so that $\tfrac{1}{2}\ \underline{x}^T \underline{\underline{A}}\, \underline{x}$ gives the quadratic part of (17). The vector $\underline{b}$ can be easily found so that $\underline{b}^T \underline{x}$ gives $\dot{P}$. Thus Eq. (25a) is equivalent to (17). Designating the inequality in Eq. (25c) as a strict equality, forming the matrix $\underline{\underline{C}}$ such that $\underline{\underline{C}}^T \underline{x}$ forms the left hand sides of the equilibrium equations (20), and setting vector $\underline{d}$ equal to the zero vector matches (25c) to (20). Finally, (25b) can be matched to (23) by setting components of $\underline{u}$ and $\underline{\ell}$ to $+\infty$ and $-\infty$, respectively, when (23) is not imposed. If Eq. (23) is needed, i.e. a moment is at

its yield value, then the appropriate component(s) of $\underline{u}$ or $\underline{\ell}$ are set to zero. The examples in Appendices A and B show details of writing Eqs. (17), (20), and (24) in the form of equations (25).

5. Using BEQUAD. Clearly, deriving the defining equations for a particular grid problem and presenting the necessary information to a Quadratic Program would take a considerable amount of work. Thus, the need for BEQUAD.

BEQUAD finds the equations of a given grid problem and calls upon a group of Quadratic Subroutines to solve the equations. Computation continues until $\dot{P}$ is found to be zero. That is, the program loads the grid until the collapse load is reached. BEQUAD is designed for use on the University of Minnesota timeshare system (MNFTS).

As soon as BEQUAD is called, it will begin to query the user for the necessary input. Basically, this information must define the size and spacing of the grid, material properties, the boundary conditions, the loading, the values of M_0 and M'_0, and the symmetries. BEQUAD will ask for this information with specific questions which are designed to be self-explanatory.

We can most clearly discuss the input in relation to an example. To this end we consider the grid shown in Fig. (7). The top edge is clamped, the side edges are simply supported, and the bottom edge is a free crossbeam. All beams are rectangular and made of carbon steel with a yield stress $\sigma_0 = 50 \times 10^3$ psi and a height of 1 inch. The horizontal beams are 1.2 inches wide and the vertical ones are 2.0 inches wide. It follows from Eq. (23a) that

M_0 = 15,000 lb-in. M'_0 = 25,000 lb-in.

Young's modulus is 3×10^7 psi and the moment of inertia for horizontal beams is .1 in^4 and .1667 in^4 for vertical beams. The two interior nodes are each loaded with 200 pounds and no load is applied to the bottom nodes on the cross beam.

Section 6 shows the actual computer input and output for this example to which we have only added circled numbers to use as reference. We will comment on specific points in relation to some of these numbers.

(2) The computer provides these dark squares so that the password remains private.

(7) When two numbers are called for, they may be separated by a comma, one or more blank spaces, or both.

(8) Young's modulus and moment of inertia for horizontal beams are entered first.

(9) If the response had been 0, the next question would have asked for the value of the uniform load.

(11) A 1 is entered only if (a) the grid spacing is symmetric, (b) the right and left boundaries are the same, and (c) the loads are symmetric. Each symmetry option reduces the problem to about half its previous size. In fact, the problem which is actually solved is the left half of the original as shown in Fig. 7b. The program automatically does the renumbering of nodes 4 and 6 to allow for the symmetric right-hand boundary. However, the user must only enter loads which appear in this smaller half-grid. Note that with vertical symmetry we use the left half, with horizontal symmetry we would use the top half, and with both symmetries we would use the top

left quarter.

(13) This type of question will be asked for each degree of symmetry.

(14) This question will occur only if a 1 was entered in question (9) otherwise the computer will skip to question (16). Notice that there is only 1 load in the half-grid left after symmetry.

(15) If the answer to (14) were N, this question would be repeated N times.

(21) This question only refers to the original complete grid. Since vertical symmetry was assigned, the second and third numbers must be the same.

(22) If 5 had been entered the user would have been asked how many supports, and their location. Again, the user must only enter the supports which appear in the smaller half-grid.

(23) All input has now been given for BEQUAD. The computer now runs the problem and prints the output. A complete moment solution and load factor is given for each time a moment reaches yield. The rates are not printed.

(24) Iteration 1 is fully elastic. It ends when the horizontal moment in row 3, column 2 reaches its yield value of 15,000 lb-in. The load factor is 9.80 and all other moments are below yield.

(25) During iteration 2 M_{32} remains at 15,000; all other moments are elastic. When p = 10.03, the vertical moment M'_{12} reaches negative yield, -25,000 lb-in.

(26) Finally, in iteration 3 $M_{2,2}$ reaches yield, but the other value remain constant.

(27) The problem is now complete. If another problem is to be solved, the user again types RN and hits CR (Carriage Return). If this is the only or last problem the user types BYE and hits CR.

6. Example. We present here the actual computer input and output for the example discussed in the previous section. The program was run interactively.

Computer responses have been hand-labelled with circled numbers for cross-reference to Sec. 4. After the computer has completed an instruction or question, it returns the carriage to a new line and types a question mark (?). The numbers following each (?) are typed in by the user in response to the question. The only other user - supplied parts of the following output are the user code following the colon in 1, the user password typed over by the dark squares in 2, the words MNFTS, Old, PATQUAD following the colon in 3, the time setting in 4 (the number 100 may be increased if necessary), the acquiring of the math package LINPACK in 5, and the two letter command to run the program in 6. After each user response the "carriage-return" (cr) key should be hit to return control to the computer.

582947

```
81/12/28. 10.58.55. TERMINAL: 172, P166
UOFM CYBER 730 NOS 1.3 (12/27-CO).
FAMILY (C74 OR C172): C172
1 USER NUMBER: FUN6090
PASSWORD
2 ■■■■■■■■
TERMINAL:  172, P166/TTY
USERS, TYPE *WRITEUP(NOTE)* 81/12/28.
3 RECOVER /SYSTEM: MNFTS,OLD,PATQUAD
READY.
4 SETTL(100)
READY.
5 X,FETCH(LINPACK/V=MNF)
READY.
6 RN
7 ENTER THE VERTICAL YIELD MOMENT,HORIZONTAL YIELD MOMENT
? 25000,15000
8 ENTER YOUNG'S MODULUS AND THE APPROPRIATE MOMENT OF INERTIA
 FOR HORIZONTAL AND VERTICAL BEAMS
? 3E7,.1,3E7,.1667
 IF THE LOAD IS UNIFORM ENTER THE INTEGER 0.
9 IF NOT ENTER THE INTEGER 1
? 1
10 ENTER THE NUMBER OF NODES ALONG THE TOP
AND THE NUMBER OF NODES ALONG THE SIDE
? 4,3
11 IF THE GRID CONTAINS SYMMETRY ACROSS A VERTICAL AXIS
 ENTER A 1. IF NOT ENTER A 0
? 1
12 IF THE GRID CONTAINS SYMMETRY ACROSS A HORIZONTAL AXIS
 ENTER A 1. IF NOT ENTER A 0
? 0
13 IF THE NUMBER OF NODES ALONG THE TOP IS ODD
 ENTER A 1. IF NOT ENTER A 0
? 0
14 ENTER THE NUMBER OF NON-ZERO LOADS
? 1
15 ENTER THE ROW, THE COLUMN, AND THE LOAD APPLIED THERE
? 2,2,200
16 IF THE LENGTHS ALONG THE TOP ARE CONSTANT
 ENTER A 1. IF NOT ENTER 0
? 1
17 ENTER THE CONSTANT LENGTH
? 24
18 IF THE LENGTHS ALONG THE LEFT SIDE ARE CONSTANT
 ENTER A 1. IF NOT ENTER 0
? 0
19 ENTER THE BAR LENGTH BETWEEN ROWS   1 AND   2
? 36
20 ENTER THE BAR LENGTH BETWEEN ROWS   2 AND   3
? 12
 ASSIGNMENT NUMBERS FOR THE TYPE OF BOUNDARY CONDITIONS ARE
 1 - SIMPLY SUPPORTED
 2 - CLAMPED
 3 - FREE WITH CROSS BEAM
 4 - FREE CANTILEVER
21 ENTER THE ASSIGNMENT NUMBERS FOR THE TOP, LEFT,
 RIGHT,AND THE BOTTOM BOUNDARIES.
? 2,1,1,3
22 IF THE CORNER OF AN INTERSECTION OF TWO TYPE 3 BOUNDARIES
 HAS A SUPPORT ENTER 5. IF NOT ENTER 0
? 0
```

582948

23 ITERATION 1

UNKNOWN HORIZONTAL MOMENTS	ROW	COLUMN
10974.80504	2	2
15000.00000	3	2

24

UNKNOWN VERTICAL MOMENTS	ROW	COLUMN
-24077.77778	1	2
7500.00000	2	2

THE LOAD FACTOR P IS 9.79722

ITERATION 2

25

UNKNOWN HORIZONTAL MOMENTS	ROW	COLUMN
11472.70546	2	2
15000.00000	3	2

UNKNOWN VERTICAL MOMENTS	ROW	COLUMN
-25000.00000	1	2
7500.00000	2	2

THE LOAD FACTOR P IS 10.02904

26 ITERATION 3

UNKNOWN HORIZONTAL MOMENTS	ROW	COLUMN
15000.00000	2	2
15000.00000	3	2

UNKNOWN VERTICAL MOMENTS	ROW	COLUMN
-25000.00000	1	2
7500.00000	2	2

THE LOAD FACTOR P IS 10.76388

27 END OF REPORT

SRU 6.645 UNTS.

RUN COMPLETE.

7. Results. The solution at each "time" is printed as in the example in Sec. 6. The moments are identified by their row and column. Fig. 13 shows how a grid is identified in terms of rows and columns.

A number of problems have been solved. Table 1 gives results obtained from BEQUAD, BEAMPLT [3] (a linear programming routine for the perfectly plastic solution of the grid problem), and in some cases, from theory (results taken from Ref. [4]). P_c is used to identify the value of the collapse load. P_e corresponds to the first load at which one or more moments reach their yield point (i.e. elastic limit). The first four cases were a 3 by 3, a 4 by 4, a 5 by 5, and a 6 by 5 grid. These were uniformly loaded with simply supported boundaries. Figure 8 shows the moments which have reached yield and the grid deformation profiles.

A 5 by 5, a 6 by 5, and a 6 by 6 grid, all with a load applied at the second row and second column, and simply supported boundaries, were also run. Figure 9 shows results. Figure 10a shows a 6 by 6 grid with $M_0 \neq M'_0$, and non-uniform spacing. The same grid, but non-uniform loading is shown in Fig. 10b. Finally, Fig. 11 has the results of a 6 by 6 grid with clamped boundaries and a load applied at the second row and third column.

The figures identify those moments which have reached their yield point at collapse with a circle or square. A circle means the top of the beam is in compression and a square means the top is in tension. Notice that yield hinges can form only at yield moments, but that not all yield moments have hinges.

Grid size	BEQUAD		BEAMPLT	Theory
	F_t	F_c	F_c	F_c
3x3) Simply Supported	4.00	4.00	4.00	4.00
4x4) Simply Supported	2.00	2.00	2.00	2.00
5x5) S. S.	1.172	1.00	0.999	1.00
6x5) S. S.	.6107	0.833	0.833	0.833
5x5) S. S. pt. load (Fig. 9)	3.89	5.333	5.333	
6x5) S. S. (Fig.9)	3.88	5.625	5.623	
6x6) S. S. (Fig.9)	3.91	5.714	5.714	
6x6) S. S. $M_0 \neq M_0'$ (Fig.10a)	7.37	9.333	9.335	
6x6)S. S. (Fig.10b)	11.52	15.25	15.25	
6x6) Clamped (Fig. 11)	3.41	8.00	7.999	

Table I Comparison of results

References

1. H. J. Greenberg; Complementary minimum principles for an elastic-plastic material, Q. Appl. Math. 7, 85-95, 1949.
2. J. N. Goodier and P. G. Hodge, Jr.: "Elasticity and Plasticity", J. Wiley & Sons, N.Y. 1958.
3. P. G. Hodge, Jr. and P. Tait, "BEAMPLT: A Program for Finding the Yield-Point Load of Transversely Loaded Rectangular Grids", Report AEM-H1-26, University of Minnesota, 1981.
4. P. G. Hodge, Jr.: "Plastic Analysis of Structures", McGraw-Hill Book Co., New York, 1959; Krieger Publ. Co., Malabar, FL., 1981.
5. R. Fletcher: "A FORTRAN Subroutine For General Quadratic Programming", Theoretical Physics Division, Atomic Energy Research Establishment, Harwell, England, June, 1970.

Appendix A

Conversion of Grid Problem to Quadratic Programming Problem

To convert the grid problem to a Quadratic Programming problem, as done in Sec. 4, requires every unknown to be defined in terms of a vector component x_j. The details of how this is done are presented here.

For an example we shall use the 4 by 4 grid, with simply supported top boundary, free cross beam on the sides, and free cantilever on the bottom as shown in Fig. 12. We consider the horizontal rate moments first and number them by rows (top to bottom) and columns (left to right). We skip all moments which are known to be zero, hence in this example there are only four unknown (rate) moments, numbered 1 through 4 as shown in Fig. 12. We continue by numbering the unknown vertical (rate) moments (5-12 in this example).

This type of numbering system can be done for all grids. Now, it is very easy to define a vector. If we abbreviate an unknown horizontal (rate) moment HM#, and an unknown vertical (rate) moment VM#, we then define a vector as follows

x_1 = HM1	x_5 = VM5
x_2 = HM2	x_6 = VM6
.	.
.	.
.	.
x_4 = HM4	x_{12} = VM12

$x_{13} = \dot{P}$ (P is the load factor)

For this example Eq. (17) gives

$$\begin{aligned}
\Lambda_c = {} & 2E\frac{1}{I_{zz}}\Big[\frac{L_1}{3}\dot{M}_{2,2}^2 + \frac{L_2}{3}(\dot{M}_{2,2}^2 + \dot{M}_{2,2}\cdot\dot{M}_{2,3} + \dot{M}_{2,3}^2) \\
& + \frac{L_3}{3}\dot{M}_{2,3}^2 + \frac{L_1}{3}\dot{M}_{3,2}^2 + \frac{L_2}{3}(\dot{M}_{3,2}^2 + \dot{M}_{3,2}\cdot\dot{M}_{3,3} + M_{3.3}^2 \\
& + L_{3/3}\dot{M}_{3,3}^2\Big] \\
& + 2E'\frac{1}{I'_{zz}}\Big[\frac{L'_1}{3}\dot{M}'^2_{2,1} + \frac{L'_2}{3}(\dot{M}'^2_{2,1} + \dot{M}'_{2,1}\cdot\dot{M}'_{3,1} + \dot{M}'^2_{3,1}) + \frac{L'_3}{3}\dot{M}'^2_{3,1} \\
& + \frac{L'_1}{3}\dot{M}'^2_{2,2} + \frac{L'_2}{3}(\dot{M}'^2_{2,2} + \dot{M}'_{2,2}\cdot\dot{M}'_{3,2} + \dot{M}'^2_{3,2}) \\
& + L'_{3/3}\dot{M}'^2_{3,2} + L'_{1/3}\dot{M}'^2_{2,3} + L'_{3/3}\dot{M}'^2_{3,3} \qquad (26) \\
& + L'_{2/3}(\dot{M}'^2_{2,3} + \dot{M}'_{2,3}\quad\dot{M}'_{3,3} + \dot{M}'^2_{3.3}) + L'_{1/3}\dot{M}'^2_{2,4} \\
& + L'_{2/3}(\dot{M}'^2_{2,4} + \dot{M}'_{2,4}\quad\dot{M}'_{3,4} + \dot{M}'^2_{3,4}) + L'_{3/3}\dot{M}'^2_{3,4}\Big] \\
& - \dot{P}
\end{aligned}$$

Letting $2E = 2E' = I_{zz} = I'_{zz} = L_\alpha = L'_\beta = 1$ Eq. (26) can then be written in terms of its vector components as

$$\begin{aligned}
& 2/3\, x_1^2 + 1/3\, x_1\cdot x_2 + 2/3\, x_2^2 + 2/3\, x_3^2 + \frac{1}{3}x_3\cdot x_4 + 2/3\, x_4^2 \\
& + 2/3\, x_5^2 + 1/3\, x_5\cdot x_6 + 2/3\, x_6^2 + 2/3\, x_7^2 + 1/3\, x_7\cdot x_8 \qquad (27) \\
& + 2/3\, x_8^2 + 2/3\, x_9^2 + 1/3\, x_9\cdot x_{10} + 2/3\, x_{10}^2 + 2/3\, x_{11}^2 \\
& + 1/3\, x_{11}\cdot x_{12} + 2/3\, x_{12}^2 - x_{13}
\end{aligned}$$

From the coefficients of the quadratic terms the non-zero components of the 13 by 13 matrix $\underline{\underline{A}}$ are found to be

$$A_{1,1} = A_{2,2} = A_{3,3} = A_{4,4} = A_{5,5} = A_{6,6} = A_{7,7} = A_{8,8} = A_{9,9} = A_{10,10} = A_{11,11}$$

$$A_{12,12} = 4/3$$

$$A_{1,2} = A_{2,1} = A_{3,4} = A_{4,3} = A_{5,6} = A_{6,5} = A_{7,8} = A_{8,7} = A_{9,10} = A_{10,9}$$

$$= A_{11,12} = A_{12,11} = 1/3$$

Since $\dot{P}$ is the only linear term in Eq. (26) the only non-zero term in $\underline{b}$ is $b_{13} = 1$

A similar process is used to convert the equilibrium equations (20) to Eq. (25c). For an example of a typical equilibrium equation we look at the sixth node in Fig. 12, i.e. the node in Column 2, row 2. The equilibrium equation before conversion is

$$\frac{\dot{M}_{2,2} - \dot{M}_{2,1}}{L_1} + \frac{\dot{M}_{2,2} - \dot{M}_{2,3}}{L_2} + \frac{\dot{M}'_{2,2} - \dot{M}'_{1,2}}{L_1'}$$

$$+ \frac{\dot{M}'_{2,2} - \dot{M}'_{3,2}}{L'_2} - Pf_{2,2} = 0 \qquad (28)$$

Noting that $M_{2,1}$ and $\dot{M}'_{1,2} = 0$ because of the left and top boundary conditions, we can write (28) as

$$\frac{1}{L_1} + \frac{1}{L_2} \quad x_1 - {}^{x_2}/_{L_2} + \frac{1}{L_1'} + \frac{1}{L_2'} \quad x_7$$

$$- \frac{x_8}{L'_2} - f_{2,2}\, x_{13} = 0 \qquad (29)$$

Considering all 12 equilibrium equations, and letting all lengths and loads equal one, we find the non-zero components of the matrix $\underline{\underline{C}}$ are

$$C_{11} = C_{6,1} = C_{2,2} = C_{8,2} = C_{1,3} = C_{10,3} = C_{2,4} = C_{12,4} = C_{3,5}$$

$$= C_{5,5} = C_{4,6} = C_{7,6} = C_{3,7} = C_{9,7} = C_{4,8} = C_{11,8} = C_{6,9}$$

$$= C_{8,10} = C_{10,11} = C_{12,12} = C_{13,1} = C_{13,2} = C_{13,3} = \cdots = C_{13,12}$$

$$= -1$$

$$C_{5,1} = C_{1,2} = C_{7,2} = C_{2,3} = C_{9,3} = C_{11,4} = C_{6,5} = C_{3,6} =$$

$$C_{8,6} = C_{4,7} = C_{10,7} = C_{12,8} = 2$$

Thus we may now express Eqs. (17) and (20) in terms of (25a) and (25c).

Appendix B

Time History Process

As explained in Sec. 4, to find the "time" history of our grid problem requires solving (25) a number of times. However, the only equation which changes in each iteration is (25b). We now will discuss some of the details involved in this process.

To this end we consider a hypothetical problem with two unknown horizontal moments with a yield moment of 1.0, and two unknown vertical moments with a yield moment of 2.0. We assign the two horizontal rate moments to the vector components x_1 and x_2, and the vertical rate moments to x_3 and x_4.

Now, assume we know Eqs. (25a) and (25c) in terms of $\underline{x}$, and we also have a means of solving Eqs. (25). For the first iteration we set the components of $\underline{u}$ (in Eq. (25b) to ∞ and the components of ℓ equal to $-\infty$, i.e. the upper and lower bounds on our unknowns are set to very large positive and negative numbers respectively. Let's assume we arrive at the following solution

$$x_1 = x_2 = 1 \qquad x_3 = x_4 = -1$$

$$x_5(\dot{P}) = 1/2$$

We now integrate and find (note, initially all moments and load factor P are zero)

$$HM1 = HM2 = t \qquad VM1 = VM2 = -t$$

$$P = 1/2\ t$$

where HM0 = represents the unknown horizontal moment corresponding to its rate moment counter-part, and VM0 has a similar meaning for

vertical moments. The largest value of t, with the moments still satisfying Eqs. (100), is 1. Thus, at iteration 1 we have

Iteration 1:

$$HM1 = HM2 = 1 \qquad VM1 = VM2 = -1$$

$$P = \tfrac{1}{2}$$

Solving (hypothetically) again, but with $u_1 = u_2 = 0$ because the two horizontal moments have yielded in tension (i.e. Eq (24a) is imposed), gives

$$x_1 = x_2 = 0 \qquad x_3 = x_4 = -1$$

$$x_5 = 1$$

Integrating:

$$HM1 = HM2 = 1 \qquad VM1 = VM2 = -(t + 1)$$

$$P = t + \tfrac{1}{2}$$

Again, we find the largest value of t to be 1. Thus

Iteration 2:

$$HM1 = HM2 = 1 \qquad VM1 = VM2 = -2$$

$$P = 1.5$$

For the next iteration we would impose the restrictions $u_1 = u_2 = 0$ and $\ell_3 = \ell_4 = 0$, since the vertical moments have yielded in compression.

However, in this (hypothetical) case there is no need to solve again because every unknown moment has yielded. If we did

solve, $\dot{P}$ would be zero indicating we had reached collapse load in the previous step.

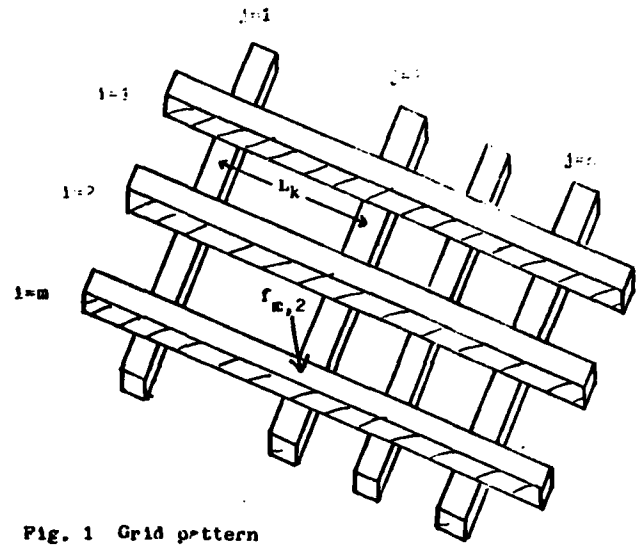

Fig. 1 Grid pattern

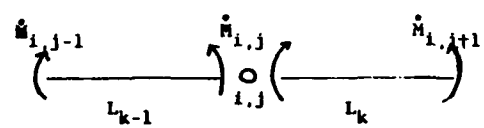

Fig. 2 Free body diagram of two horizontal beam segments at node i,j

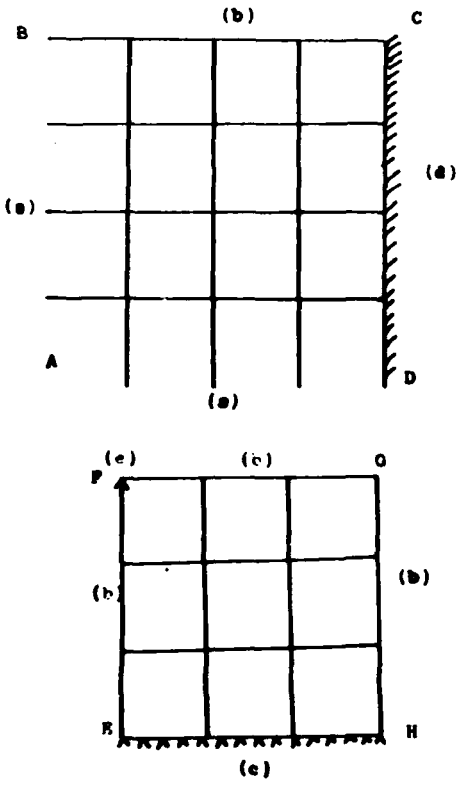

Fig. 3 Boundary conditions
(a) free cantilever

(b) free crossbeam

(c) simply supported

(d) clamped

(e) supported corner

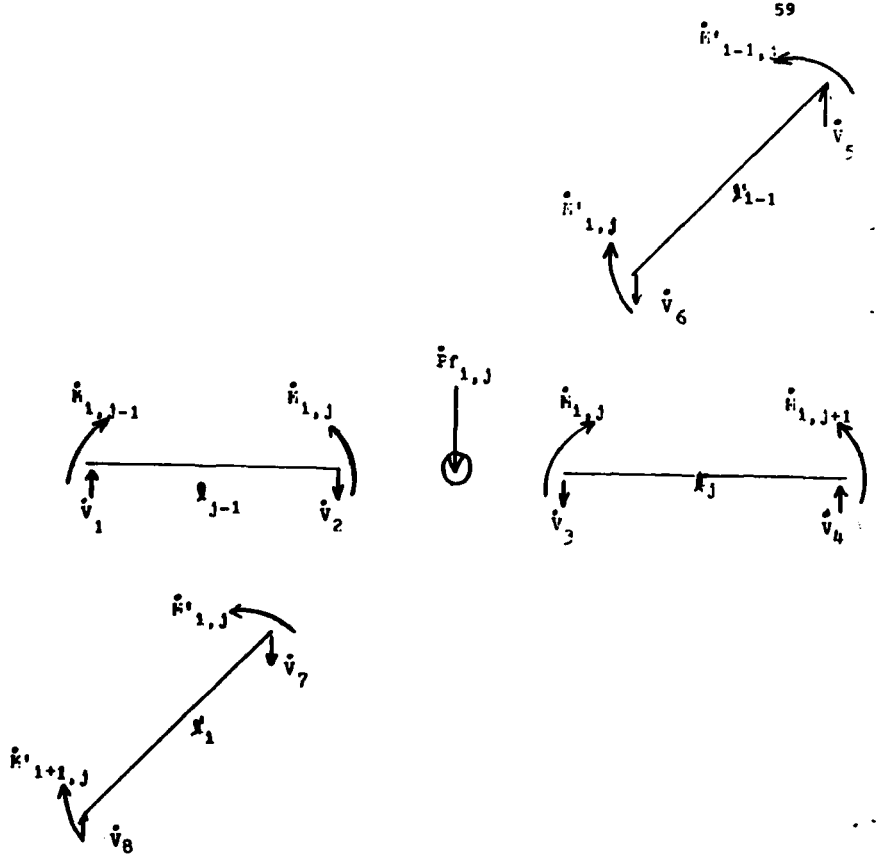

Fig. 4 Free body diagram of an interior node

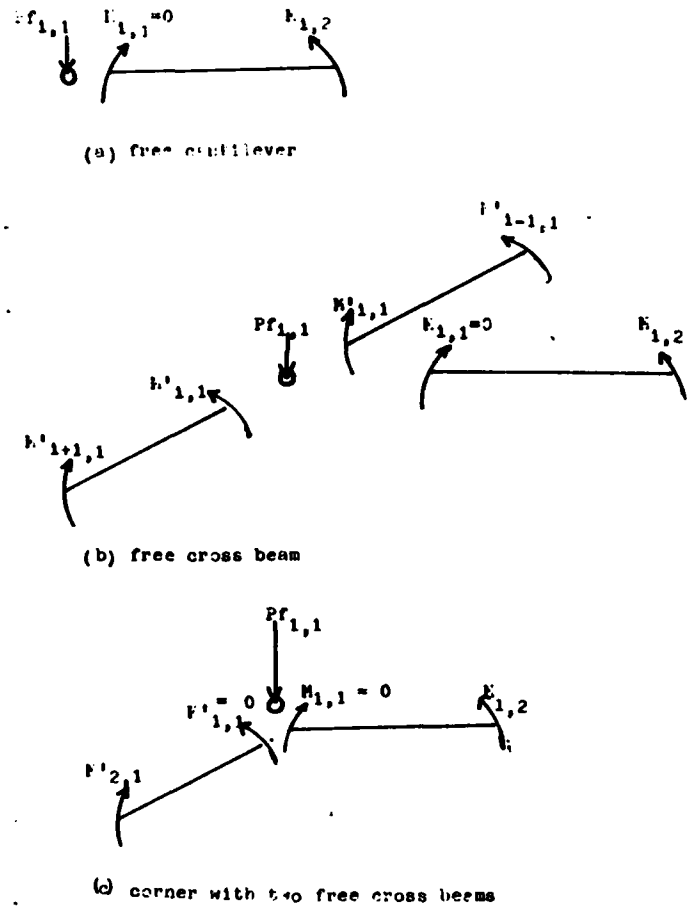

Fig. 5 Boundary relations

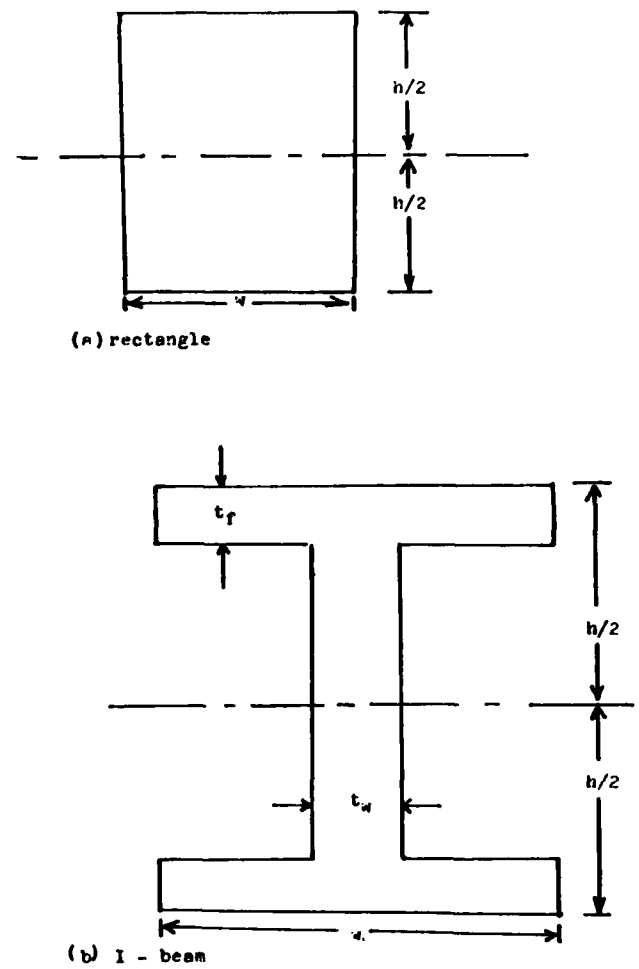

Fig. 6 X - sections

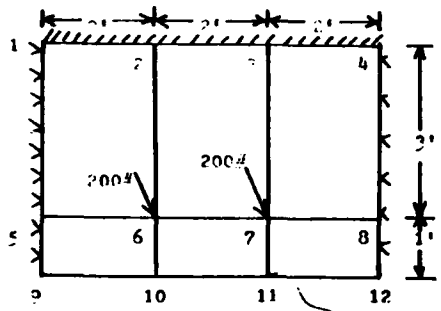

(a) original grid

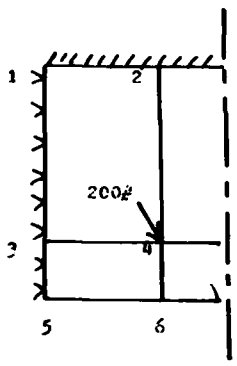

(b) smaller grid

Fig. 7 Example Problem

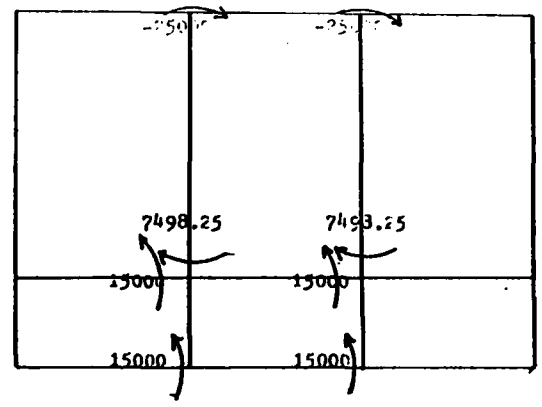

(c) results The load factor P is 10.762

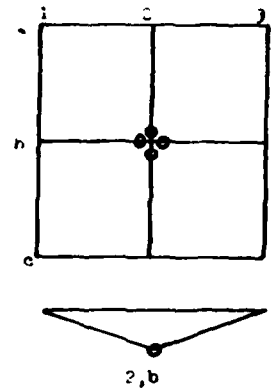

(a)

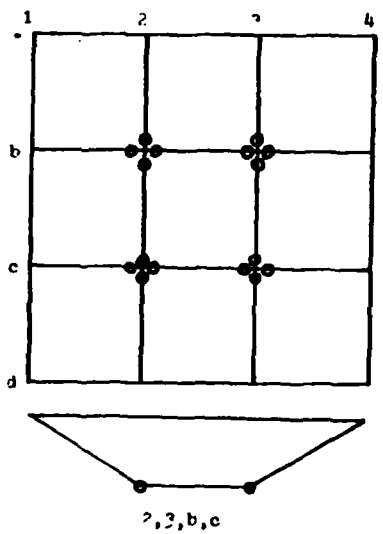

(b)

Fig. 8 Simply supported grids with a unit load applied to every interior node[2].

(a) 3 by 3 (P_c = 4; P_c/P_e = 1)

(b) 4 by 4 (P_c = 2; P_c/P_e = 1)

(c) 5 by 5 (P_c = 1; P_c/P_e = 1.172)

(d) 6 by 5 (P_c = .833; P_c/P_e = 1.364)

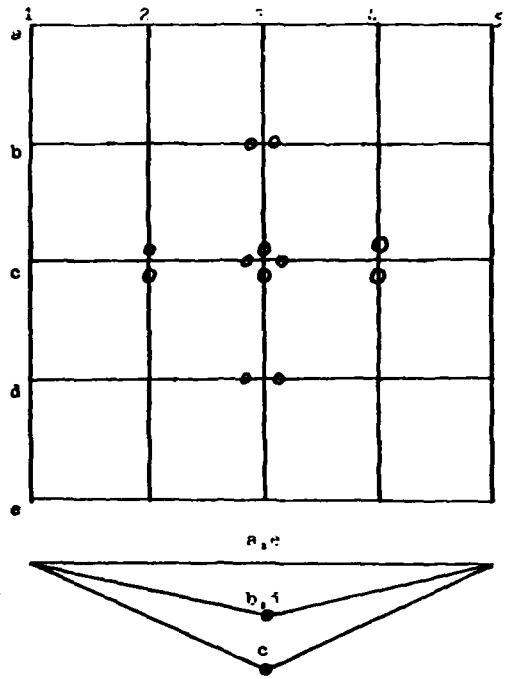

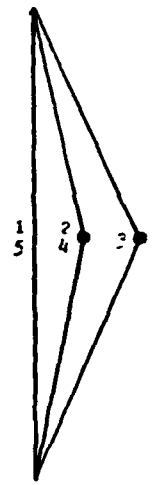

(c)

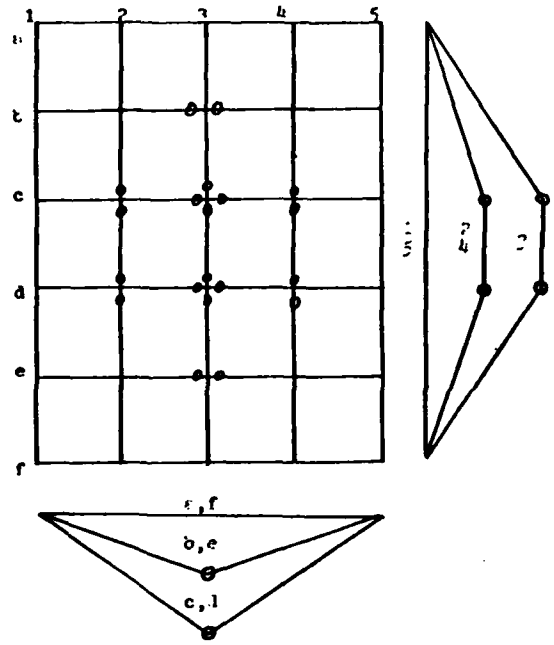

(d)

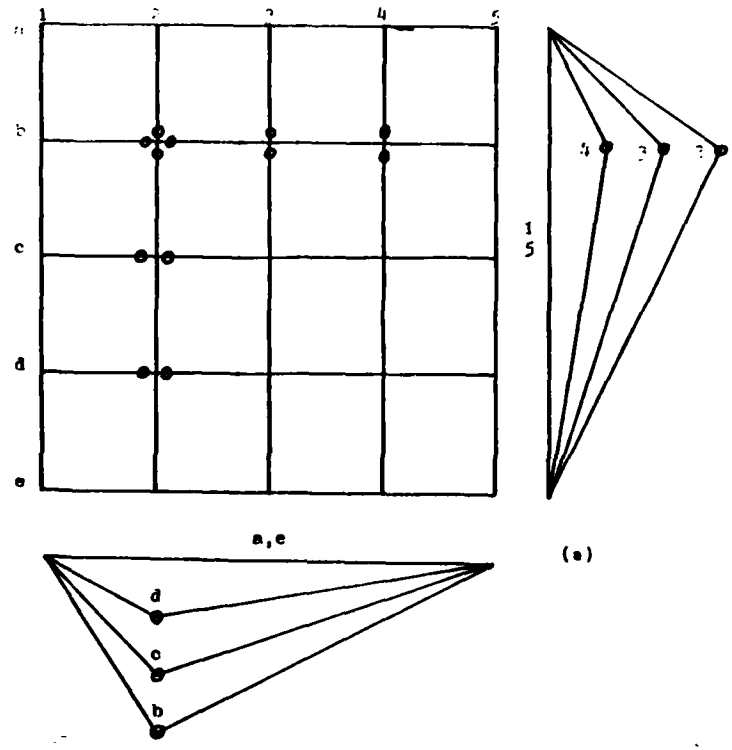

(a)

Fig. 9. Simply supported grids with [illegible] applied only to node b0. Small circles and squares represent moments equal to positive and negative yield moments, respectively.

(a) 5 by 5 (P_c = 5.333; P_c/P_e = 1.375)

(b) 6 by 5 (P_c = 5.625; P_c/P_e = 1.450)

(c) 6 by 6 (P_c = 5.714; P_c/P_e = 1.463)

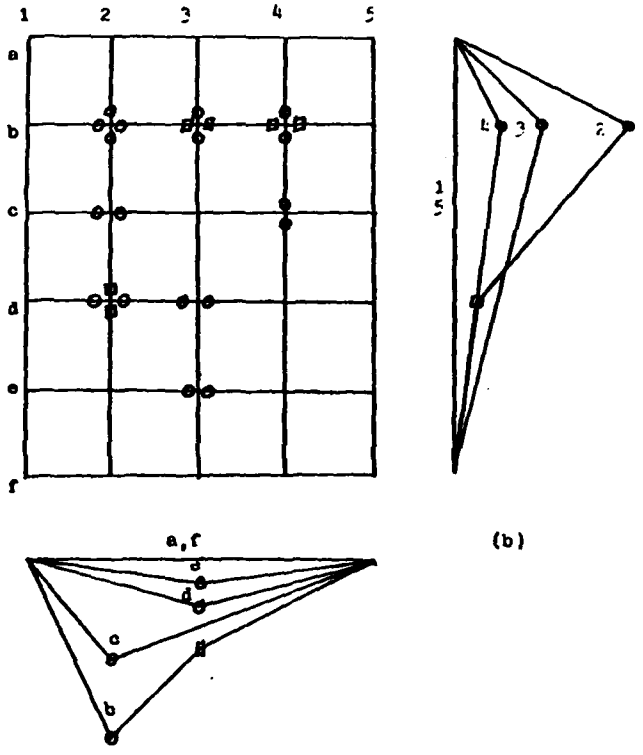

(b)

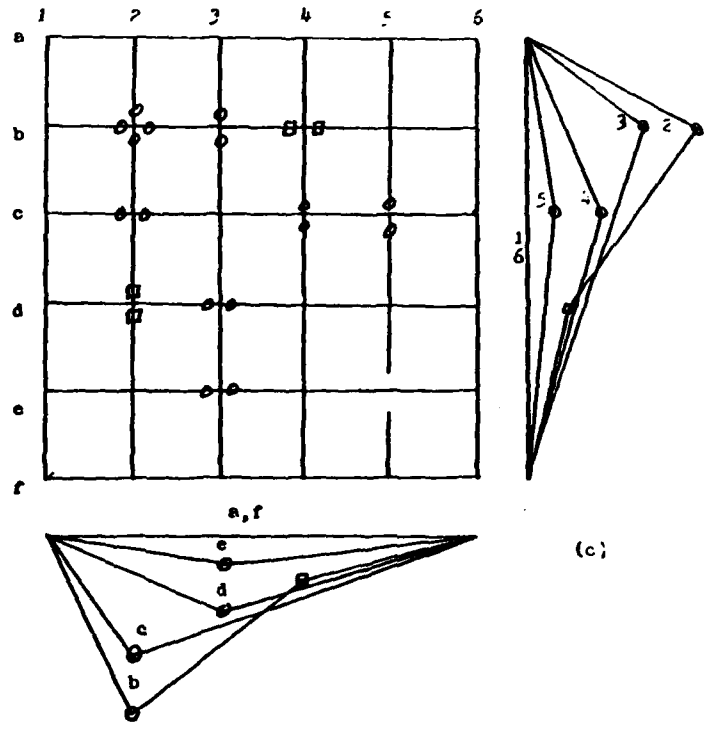

(c)

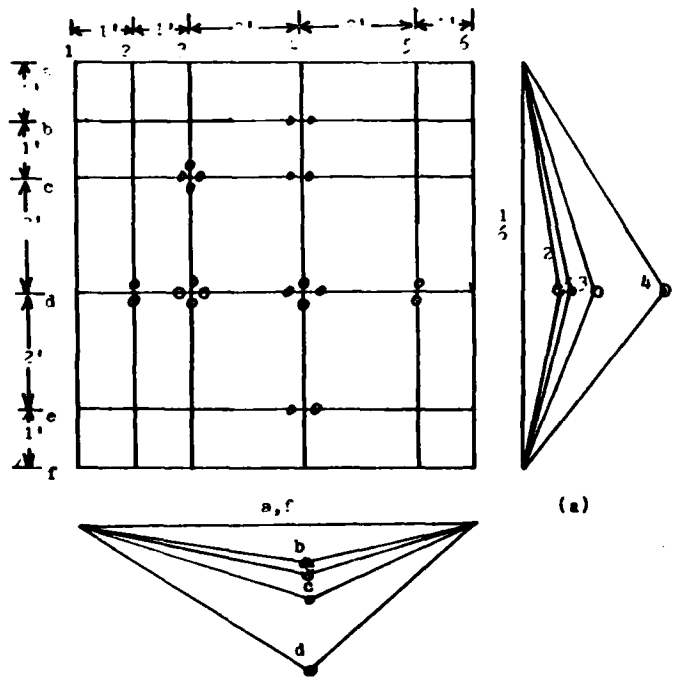

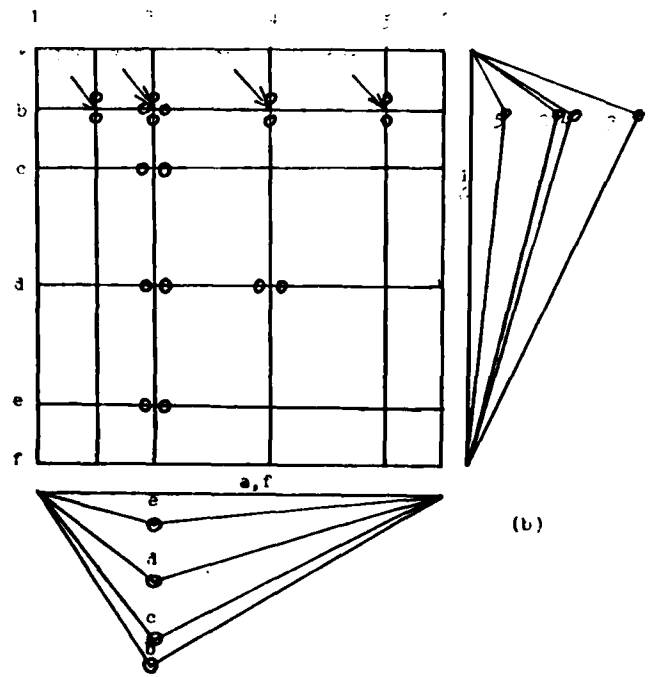

Fig. 10 6 by 6 simply-supported grid with M_0 = 15,000 lb-in,

M_0' = 25,000 lb-in, E = 3×10^7 psi, I^H_{zz} = .1 in^4, I^V_{zz} = .1667 in^4

(a) load of 100 lb at each interior node (P_c = 9.333; P_c/P_e = 1.267)

(b) loaded as shown (P_c = 15.25; P_c/P_e = 1.324)

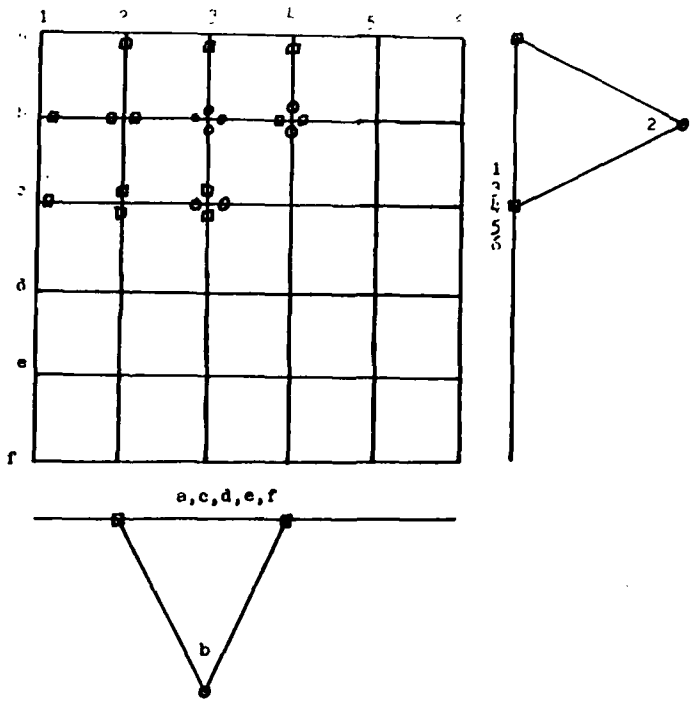

Fig. 11 Clamped 5 by 6 grid with unit load at b?

(P_c = 8; P_c/P_e = 2.347)

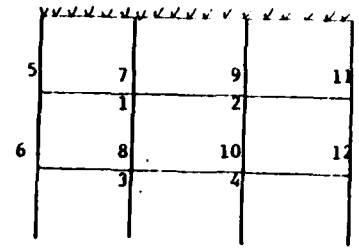

Fig. 12 Vector conversion

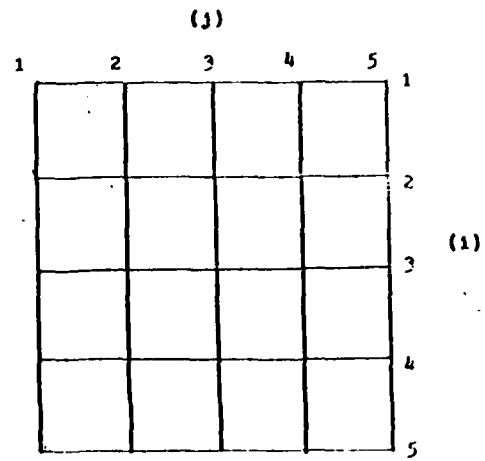

A grid can have "m" rows and "n" columns. "i" represents the ith row and "j" represents the jth column.

Fig. 13 Matrix notation system

4. SHAKEDOWN

1. Introduction.

A problem of considerable interest is that of determining the safety factor for a structure acted upon by a prescribed set of loads. One approaches the problem by making some simplifying assumptions as to how the members of the structure will be modeled. If the members are assumed to consist of an ideal rigid-plastic material then it is only necessary to consider the instantaneous collapse load, and the analysis is relatively simple. However, if we assume the structure is composed of a more realistic material, then a consideration of shakedown may need to be included in the analysis. The structure is then considered to be safe if only a limited amount of plastic work can be done on the structure by any allowable application of the loads.

It is usual to assume the structure will fail due to instantaneous, incremental, or alternating plastic collapse. The objective is to find a load domain such that for any loading path lying within this domain the structure will not collapse.

For a beam or frame made of straight, piecewise-constant sections and subject only to concentrated forces there will be only a finite number of critical points at which plastic work will be done. The situation is more complicated for a structure which is acted upon by one or more distributed loads. In this case there may be an infinite number of points at which plastic work is done. The problem is then one of optimization. For example, of all possible configurations which will cause incremental plastic collapse we choose that one which corresponds to the lowest

multiplier of the prescribed loads for which incremental plastic collapse will occur. Alternating plastic collapse is treated in a similar manner.

However, even when a load domain has been found for which the structure is safe against instantaneous, incremental, and alternating plastic collapse there remains the question of whether all possible types of collapse behavior by which the structure may fail have been taken in account. For structures acted upon only by concentrated loads the answer is yes. For structures under distributed loads the answer is not as simple. In fact, it is shown in this report that such a structure may exhibit one further type of collapse behavior which we have called continuous plastic collapse. For a general structure, it is an open question as to whether the inclusion of the possibility of continuous plastic collapse may reduce the shakedown multiplier for the prescribed loads previously determined to guard only against instantaneous, incremental, and alternating plastic collapse.

In this report we examine the ideas discussed above by considering the example of a simple frame and attempt to answer some of the questions which have been posed. In order to clearly see how the analysis proceeds the earlier sections treat the frame acted upon only by concentrated loads. In later sections the analysis is made more complicated when one of the concentrated loads is replaced by a distributed load. Nevertheless the example remains sufficiently simple to draw some conclusions as to the effect of the presence of distributed loads and to suggest lines along which future work might be directed.

Specifically, Sec. 2.1 treats the simple frame under concentrated loads and contains examples of instantaneous, incremental, and alternating plastic collapse as well as examples of loading

cycles which result in totally elastic and limited plastic behavior. Sections 2.2 and 2.3 are concerned with definitions of the shakedown domain and shakedown multiplier, and in Sec. 2.4 the shakedown domain for the frame is actually determined.

In Sections 3.1, 3.2, 3.3, and 3.4 the same frame acted upon by a distributed load is considered and examples of instantaneous, incremental, and alternating plastic collapse are given. Section 3.5 is concerned with obtaining a loading path for which the frame will fail due to continuous plastic collapse. Shakedown behavior is mentioned in Sec. 3.6. Sections 3.7 and 3.8 contain modified definitions for collapse domain and shakedown multiplier which take the additional continuous plastic collapse behavior into account. The shakedown domain for this simple frame is then determined in Sec. 3.9. Finally, in Sec. 4 some ideas for future research are discussed.

2.1 Example of a frame under concentrated loads.

We consider a pin-supported frame as shown in Fig. 1. For simplicity, it is assumed that the frame members have an ideal sandwich section and that axial forces do not affect plastic yielding. The magnitude of the yield moment at any point on the frame is M_0. We introduce dimensionless quantities defined by

$$m = \frac{M}{M_0} \qquad f_1 = \frac{F_1 L}{M_0} \qquad f_2 = \frac{F_2 L}{M_0} \tag{2.1.1}$$

where M is the moment at any point on the frame.

In the following sections it will be seen that the frame may collapse due to any one of three different types of collapse behavior namely, i) instantaneous plastic collapse, ii) incremental plastic collapse, and iii) alternating plastic collapse. The particular type of collapse which will occur depends on the actual loading program for f_1 and f_2. Each of these types of collapse behavior is best illustrated by an example. The first such example will demonstrate instantaneous plastic collapse.

2.1a Instantaneous plastic collapse.

We begin by determining a load domain such that when f_1 and f_2 follow a loading path which always remains within this domain then instantaneous plastic collapse cannot occur.

Consider the collapse mechanisms shown in Fig. 2. It can easily be shown by using the principle of virtual work that for each of the collapse mechanisms the loads must satisfy

$$f_1 = 5.333 \tag{2.1.2a}$$

$$f_2 = 2 \tag{2.1.2b}$$

$$f_2 = -2 \tag{2.1.2c}$$

$$3f_1 + 2f_2 = 16 \tag{2.1.2d}$$

$$3f_1 - 6f_2 = 16 \tag{2.1.2e}$$

$$f_1 = -5.333 \tag{2.1.2f}$$

$$3f_1 - 6f_2 = -16 \tag{2.1.2g}$$

$$3f_1 + 2f_2 = -16 \tag{2.1.2h}$$

where Eq. (2.1.2a) corresponds to the collapse mechanism shown in Fig. 2(a), etc. The resulting hexagon defined by Eqs. (2.1.2) and shown in Fig. 3 is the load domain such that for this frame any loading path which lies entirely within the domain will not cause instantaneous plastic collapse.

It is evident that any loading path for f_1 and f_2 which reaches the boundary of the domain will cause the frame to suffer instantaneous plastic collapse. As an example of one such loading path we consider path OAB in Fig. 3 and carry out a complete analysis of the frame up to the point of collapse.

By considering the free-body diagram shown in Fig. 4 we can show that the moments along the frame are given in terms of a single redundant by

$$m = \begin{cases} -Hy & \text{between 5 and 1} \\ -H + (1/4f_1 - 1/2f_2)x & \text{between 1 and 2} \\ -H + (1/4f_1 - 1/2f_2)x - f_1(x - 3/2) & \text{between 2 and 3} \\ -Hy - f_2y & \text{between 3 and 4} \end{cases} \tag{2.1.3a}$$

By means of (2.1.3) the elastic energy for the frame may be determined. Minimizing the elastic energy with respect to the reaction H, we find

$$H = 3f_1/64 - f_2/2 \tag{2.1.3b}$$

and hence obtain the elastic solution

$$m = \begin{cases} (1/2f_2-3/64f_1)y & \text{between 5 and 1} \\ (1/2f_2-3/64f_1) + (1/4f_1-1/2f_2)x & \text{between 1 and 2} \\ (1/2f_2-3/64f_1) + (1/4f_1-1/2f_2)x - f_1(x-3/2) & \text{between 2 and 3} \\ -(1/2f_2+3/64f_1)y & \text{between 3 and 5} \end{cases} \tag{2.14}$$

For this frame there are three critical moments to be considered, at the points numbered 1, 2, and 3. From (2.1.3) we obtain

$$\begin{aligned} m_1 &= -H \\ m_2 &= -H + 3/2(1/4f_1-1/2f_2) \\ m_3 &= -H - f_2 \end{aligned} \tag{2.15}$$

and from the elastic solution (2.1.4) the critical moments are

$$m_1 = 1/2f_2 - 3/64f_1$$
$$m_2 = -1/4f_2 + 21/64f_1 \qquad (2.1.6)$$
$$m_3 = -1/2f_2 - 3/64f_1$$

Setting $f_2 = 0$ in Eqs. (2.1.6) and increasing f_1, we find that the elastic solution holds until

$$f_1 = 64/21 = 3.048 \qquad (2.1.7)$$

and at this point the moments are given by

$$m_1 = m_3 = -0.143 \qquad m_2 = 1 \qquad (2.1.8)$$

As f_1 is further increased we may regard the frame as an elastic structure with a perfect hinge at the point 2 acted upon by the additional load. The quantities involved in this auxiliary problem are denoted by bars. The solution is determined from Eqs. (2.1.5) from which we find

$$\bar{m}_1 = \bar{m}_3 = -3/8\bar{f}_1 \qquad \bar{m}_2 = 0 \qquad (2.1.9)$$

We choose to stop increasing f_1 when it equals 4.5. At this point, we have

$$\bar{f}_1 = 1.452 \qquad \bar{m}_1 = \bar{m}_3 = -0.545 \qquad \bar{m}_2 = 0 \qquad (2.1.10)$$

Eqs. (2.1.9) together with Eqs. (2.1.10) give the complete solution

$$f_1 = 4.5 \qquad f_2 = 0 \qquad m_1 = m_3 = -0.688 \qquad m_2 = 1 \qquad (2.1.11)$$

We now hold $f_1 = 4.5$ and increase f_2. The elastic equations (2.1.6) show that an increase in f_2 will decrease m_2. Therefore the frame returns to fully elastic behavior and is governed by Eqs. (2.1.6). Again using bars to denote additions to the quantities in Eqs. (2.1.11) we have

$$\bar{f}_1 = 0 \qquad \bar{m}_1 = 1/2\bar{f}_2 \qquad \bar{m}_2 = -1/4\bar{f}_2 \qquad m_3 = -1/2\bar{f}_2 \qquad (2.1.12)$$

Therefore, the complete solution is

$$f_1 = 4.5 \qquad f_2 = \bar{f}_2 \qquad m_1 = -0.688 + 1/2\bar{f}_2$$
$$m_2 = 1 - 1/4\bar{f}_2 \qquad m_3 = -0.688 - 1/2\bar{f}_2 \qquad (2.1.13)$$

This solution holds until $f_2 = 0.625$ at which point $m_3 = -1$ and the solution is

$$f_1 = 4.5 \qquad f_2 = 0.625 \qquad m_1 = -0.376$$
$$m_2 = 0.844 \qquad m_3 = -1 \qquad (2.1.14)$$

As f_2 is increased further we again consider an auxiliary problem but this time the perfect hinge is at the point 3. The auxiliary solution is

$$\bar{f}_1 = 0 \qquad \bar{m}_1 = \bar{f}_2 \qquad \bar{m}_2 = 1/4\bar{f}_2 \qquad \bar{m}_3 = 0 \qquad (2.1.15)$$

The complete solution is

$$f_1 = 4.5 \qquad f_2 = 0.625 + \bar{f}_2$$
$$m_1 = -0.375 + \bar{f}_2 \qquad m_2 = 0.844 + 1/4\bar{f}_2 \qquad m_3 = -1 \qquad (2.1.16)$$

It is seen that this solution holds up to $\bar{f}_2 = 0.625$ at which point $m_3 = 1$ and the frame is now in the collapse mechanism shown in Fig. 2(d). The complete solution at this point is

$$f_1 = 4.5 \qquad f_2 = 1.25 \qquad m_1 = 0.249 \qquad m_2 = 1 \qquad m_3 = -1 \qquad (2.1.17)$$

Stage	1U	1L	2U	2Δ	2L	3U	3Δ	3L	4U	4Δ	4L
Control	$+f_1$		$+\Delta f_1$			$+\Delta f_2$			$+\Delta f_2$		
m_1	all E		$2P^+$			all E			$3P^-$		
f_1	1	3.048	1	1.452	4.5	0	0	4.5	0	0	4.5
f_2	2	0	0	0	0	1	.625	.625	1	.625	1.25
m_1	-3/64	-.143	-3/8	-.545	-.688	1/2	.312	-.375	1	.625	1
m_2	21/64	1	0	0	1	-1/4	-.156	.844	1/4	.156	-1
m_3	-3/64	-.143	-3/8	-.545	-.688	-1/2	-.312	-1	0	0	
terminate	$2P^+$		$f_1=4.5$			$3P^-$			$2P^+$		

Table 1
Complete History Illustrating
Instantaneous Plastic Collapse

The loading program is summarized in Table 1. The loading path is OAB in Fig. 3. A new stage is signified each time any critical moment changes between elastic and plastic behavior. For each stage the column labelled U is the solution for a unit value of the control load, column Δ is the unit solution multiplied by the limiting value of the control load, and column L is the total solution at the end of that stage, i.e., the sum of column Δ and the column L of the previous stage.

2.1.b Incremental plastic collapse.

It is possible to choose a loading path for which the frame will collapse even though this loading path always remains within the load domain shown in Fig. 3. As an example we consider the load path OACACA... in Fig. 3 where point C corresponds to $f_1 = 4.5$, $f_2 = 1$.

The initial stages of the loading path are the same as those for the instantaneous plastic collapse described in section 2.1.a. As before f_1 is increased to 4.5 and then f_2 is increased to 0.625. At this point the complete solution is given by Eqs. (2.1.14). f_2 is now further increased and during this stage the auxiliary solution is given by Eq. (2.1.15). Thus, Table 1 applies up through stage 4U. However, in this example we stop increasing f_2 when it has reached $f_2 = 1$. The solution for $f_2 = 1$ is

$$f_1 = 4.5 \quad f_2 = 1 \quad m_1 = 0 \quad m_2 = 0.938 \quad m_3 = -1 \qquad (2.1.18)$$

as shown in column 4L of Table 2.

Stage	1L	2L	3L	4U	4L	5U	5L	6U	6L
Control	$+f_1$	$+\Delta f_1$	$+f_2$	$+\Delta f_2$		$-\Delta f_2$		$-\Delta f_2$	
m_1	all E	$2P^+$	all E	$3P^-$		all E		$2P^+$	
f_1	3.048	4.5	4.5	0	4.5	0	4.5	0	4.5
f_2	0	0	0.625	1	1	-1	0.75	-1	0
m_1	-0.143	-0.688	-0.375	1	0	-1/2	-0.125	-3/4	-0.688
m_2	1	1	0.844	0.14	0.938	1/4	1	0	1
m_3	-0.143	-0.688	-1	0	-1	1/2	-0.875	1/4	-0.688
terminate	$2P^+$	$f_1=4.5$	$3P^-$	$f_2=1$		$2P^+$		$f_2=0$	

Table 2
Complete History Illustrating
Incremental Plastic Collapse

The next stage in the loading is to decrease f_2. Since a negative $\bar{f}_2$ will return point 3 to an elastic condition, we again use Eqs. (2.1.6). Stage 5U of Table 2 shows the unit solution for decreasing f_2. The complete solution during the unloading is

$$f_1 = 4.5 \qquad f_2 = 1 + \bar{f}_2$$
$$m_1 = 1/2\bar{f}_2 \quad m_2 = 0.938 - 1/4\bar{f}_2 \quad m_3 = -1 - 1/2\bar{f}_2 \tag{2.1.19}$$

Yielding first occurs at the point numbered 2 at a value $\bar{f}_2$=-0.25. The complete solution is

$$f_1 = 4.5 \qquad f_2 = 0.75$$
$$m_1 = -0.125 \qquad m_2 = 1 \quad m_3 = -0.875 \tag{2.1.20}$$

When f_2 is decreased further in stage 6, a positive hinge is again present at point 2, hence the unit solution is as shown in column 6U of Table 2. The complete solution during this stage is

$$f_1 = 4.5 \qquad f_2 = 0.75 + \bar{f}_2$$
$$m_1 = -0.125 + 3/4\bar{f}_2 \quad m_2 = 1 \quad m_3 = -0.875 - 1/4\bar{f}_2 \tag{2.1.21}$$

From these equations we see that no further yielding takes place as f_2 is decreased to zero. At f_2=0 the solution is

$$f_1 = 4.5 \qquad f_2 = 0$$
$$m_1 = -0.688 \qquad m_2 = 1 \qquad m_3 = -0.688 \tag{2.1.22}$$

as shown in column 6L of Table 2. Since this column is identical to column 2L, it is evident that the stages 3-6 will be repeated each time the load point traverses the cycle ACA in Fig. 3. Thus if the cycle is repeated the same solutions will be obtained during this loading. We note that when each cycle has been completed plastic work has been done at the points 2 and 3. Clearly the same work will be done during each cycle. Since real materials have only a finite capacity for absorbing work, the material will fail after some finite number of cycles.

From the viewpoint of displacements, point 2 will undergo a certain discontinuity of slope $\Delta\theta_2$ during stage 6, and point 3 will undergo a certain negative discontinuity $\Delta\theta_3$ during stage 4. Other than that, all changes in slope will be continuous during the cycle, hence at the completion of one cycle ACA the only slope discontinuities will be $\Delta\theta_2$ and $\Delta\theta_3$. It can be shown that $\Delta\theta_3 = -\Delta\theta_2$. Also, it is clear that the net elastic deformation during the cycle ACA will be zero. Therefore, at the end of stage 6, the frame will deform into its shape at stage 2L plus a mechanism motion in Fig. 2(d) with a magnitude $\Delta\theta_2$. Further, this mechanism motion will be added again during each cycle, so that eventually the deformations would become so large as to make the frame unserviceable. In other words, after some finite number of cycles the frame will collapse.

2.1.c Alternating plastic collapse.

Another example of a loading path lying entirely within the load domain but still leading to collapse of the frame is illustrated by path OADADA... in Fig. 3. This is the third type of collapse behavior and is called alternating plastic collapse.

The loading path is as follows; increase f_1 to 4.5, then decrease f_1 below zero to a value of -4.5, finally increase f_1 to 4.5 again. The results are summarized in Table 3. On examination of this table it can be seen that the moments at the end of the cycle when f_1 has returned to a value of 4.5 are the same as those which held at the start. Thus repetition of this loading cycle results in a hinge forming only at the point numbered 2. However, unlike the hinges in the case of incremental plastic collapse the yield moment at this hinge alternates in sign during each cycle. For the ideal material considered here, a certain negative slope discontinuity $-\Delta\theta$ would occur in stage 4, but a positive discontinuity of the same magnitude would occur in stage 6. Therefore, at the end of a cycle AOA the shape of the frame would be unchanged. However, both the changes $-\Delta\theta$ in stage 4 and $+\Delta\theta$ in stage 6 correspond to positive work being done on the frame. Since any real material has only a finite capacity to absorb work, the frame would break at point 2 after some finite number of cycles. Thus this cycle also would result in a form of plastic collapse.

Table 3

Complete History Illustrating

Alternating Plastic Collapse

Stage	1L	2L	3U	3Δ	3L	4U	4Δ	4L	5U	5L	6U	6L
Control	$+f_1$	$+\Delta f_1$	$-\Delta f_1$			$-\Delta f_1$			$+\Delta f_1$		$+\Delta f_1$	
m_1	all E	$2P^+$	all E			$2P^-$			all E		$2P^+$	
f_1	3.048	4.5	-1	-6.095	-1.595	-1	-2.905	-4.5	1	1.595	1	4.5
f_2	0	0	0	0	0	0	0	0	0	0	0	0
m_1	-0.143	-0.688	3/64	0.286	-0.402	3/8	1.089	0.688	-3/64	0.402	-3/8	-0.688
m_2	1	1	-21/64	-2	-1	0	0	0	21/64	1	0	1
m_3	-0.143	-0.688	3/64	-0.286	-0.402	3/8	1.089	0.688	3/64	0.402	-3/8	-0.688
terminate	$2P^+$	$f_1=4.5$	$2P^-$			$f_1=-4.5$			$2P^+$		$f_1=4.5$	

2.1.d Totally elastic behavior.

Clearly, if f_1 and f_2 remain sufficiently small, the frame will always remain elastic. As a trivial example, consider the load path OEFGOEFGO... in Fig. 3, where F is the load state $f_1=2$, $f_2=1$. Table 4 shows the results. Since columns 5L and 1L are identical, the same elastic behavior will continue indefinitely.

2.1.e Limited plastic behavior.

A final possible behavior for the frame is a loading cycle in wh' a finite amount of plastic flow occurs near the beginning foll wd by purely elastic behavior. As an example, consider the path OAHIOAHIO... where H is the load state $f_1=4.5$, $f_2=0.625$. Table 5 shows the results. Through stage 3 this example is the same as that shown in Table 1, where m_2 was plastic during stage 2. Although m_3 just reaches yield at the end of stage 3, it immediately unloads in stage 4 so that no plastic flow has taken place. Similarly, at the end of stage 6, m_2 just reaches yield but it will again unload immediately in stage 7. Since stage 6L is identical to stage 2L, further cycles AHIO will always be elastic.

2.2 Shakedown.

If the frame engages in only a limited amount of plastic flow we say that it "shakes down" to elastic behavior and refer to the cycle as a <u>shakedown</u> cycle. Fully elastic behavior is a special case of shakedown in which the limited plastic flow is zero. In general, a frame which shakes down will remain serviceable through an extremely large number of load cycles.

Stage	1L	2L	3L	4L	5L
f_1	2	2	0	0	2
f_2	0	1	1	0	0
m_1	-0.094	0.406	0.5	0	-0.094
m_2	0.656	0.406	-0.25	0	0.656
m_3	-0.094	-0.594	-0.5	0	-0.094

Table 4

Complete History Illustrating

Totally Elastic Behavior

Stage	1L	2L	3L	4U	4L	5U	5L	6U	6L
Control	$+f_1$	$+\Delta f_1$	$+\Delta f_2$	$-\Delta f_1$		$-\Delta f_2$		$+\Delta f_1$	
m_1	all E	$2P^+$	all E	all E		all E		all E	
f_1	3.048	4.5	4.5	-1	0	0	0	1	4.5
f_2	0	0	.625	0	.625	-1	0	0	0
m_1	-.143	-.688	-.375	3/64	-.164	-1/2	-.477	-3/64	-.688
m_2	1	1	.844	-21/64	-.633	1/4	-.477	21/64	1
m_3	-.143	-.688	-1	3/64	-.789	1/2	-.477	-3/64	-.688
terminate	$2P^+$	$f_1=4.5$	$f_2=.625$	$f_1=0$		$f_2=0$		$f_1=4.5$	

Table 5

Complete History Illustrating

Shakedown

For the other three load cycles illustrated in Sec. 2.1, the frame will collapse and become unserviceable after a small number of cycles - less than 1 in the case of instantaneous collapse. This undesirable behavior is always characterized by the fact that the frame is called upon to absorb an indefinitely large amount of plastic energy.

In the example considered it is evident that any load cycle which results in indefinitely large plastic work may be characterized as either alternating collapse or incremental collapse (of which instantaneous collapse may be considered a special case). Indeed, since the moment is linear between each pair of numbered points, m_1, m_2, and m_3 are the only moments which can become plastic, hence infinite total work means infinite work at at least one of these three locations. If one or more of these points engages in both positive and negative plastic rotations, the frame will engage in alternating collapse. The only alternative is that at least one plastic hinge has an indefinitely large rotation. Since elastic deformations are bounded, this large rotation cannot take place at only one hinge, but must occur in two or more hinges so as to produce one of the mechanism patterns in Fig. 2.

Therefore, in the present example, and for any other frame which consists of piecewise constant members and is subjected only to concentrated loads, the behavior of the frame can be characterized as one of the following: shakedown, alternating collapse, or incremental collapse.

Consider next the problem in which we are given only a domain D of loads, and the actual load history may be any load-path within D. If <u>all</u> loading paths in D result in shakedown, we refer to D as a shakedown domain, but if there exists <u>any</u> cycle in D which does not produce shakedown, D is a collapse domain.

In order to keep the following discussion simple, we will consider only a special subclass of load domains, defined by two loads f_1 and f_2 which are restricted to satisfy

$$0 \le f_1 \le f_1^* \qquad -f_2^* \le f_2 \le f_2^* \tag{2.2.1}$$

where f_1^* and f_2^* are assigned extreme magnitudes for f_1 and f_2 respectively.

2.3 Shakedown multiplier.

Given a load domain D as defined by inequalities (2.2.1) we can define a field B of load domains by demanding that the loads f_1 and f_2 satisfy the inequalities

$$0 \le f_1 \le \phi f_1^* \qquad -\phi f_2^* \le f_2 \le \phi f_2^* \tag{2.3.1}$$

For any particular value of ϕ the load domain defined by inequalities (2.3.1) will be denoted D_ϕ. It should be noted that for any load domain in the field B, the ratio of the extreme magnitude of f_1 to the extreme magnitude of f_2 is always the same.

We introduce the shakedown multiplier ϕ_s which has the properties; i) for any $\phi < \phi_s$, D is a shakedown domain and ii) for any $\phi > \phi_s$, D is a collapse domain.

In the next section it is shown how the shakedown multiplier may be found for the frame of section 2.1.

2.4 A shakedown domain for a simple frame.

In general to find ϕ_s we must determine ϕ_{inc} which is the smallest ϕ for which incremental plastic collapse can occur and also determine ϕ_{alt} which is the smallest ϕ for which alternating plastic collapse can occur. It is easy to see that ϕ_{coll}, the smallest ϕ for which instantaneous plastic collapse can occur is always equal or greater than ϕ_{inc}. Thus ϕ_s is given by

$$\phi_s = \min(\phi_{inc}, \phi_{alt}) \tag{2.4.1}$$

At this point we introduce the idea of a residual moment distribution along the frame which will enable us to determine ϕ_s. The material discussed in the following is more fully treated in [1].

Let $M = M(s)$ be the actual moment at any point a distance s along the frame. Define the elastic moment $M^e(s)$ as that moment which would exist in a purely elastic frame subjected to the same loads. The residual moment $M^r(s)$ is then defined by

$$M^r(s) = M(s) - M^e(s) \tag{2.4.2}$$

Let the maximum and minimum values of $M^e(s)$ be denoted by $M^+(s)$ and $M^-(s)$ respectively. The shakedown moment distribution $\bar{M}(s)$ is defined by demanding that $\bar{M}(s)$ satisfies

$$-M_0 \le \bar{M}(s) + M^e(s) \le M_0 \tag{2.4.3}$$

for all $M^e(s)$ obtainable under the given loading conditions. Inequality (2.4.3) may be replaced by

$$-M_0 \le \bar{M}(s) + M^-(s) \le \bar{M}(s) + M^+(s) \le M_0 \tag{2.4.4a}$$

For the simple frame of section 2.1 this reduces in dimensionless quantities to

$$-1 \le \bar{m}_k + m_k^- \le \bar{m}_k + m_k^+ \le 1 \tag{2.4.4b}$$

for k = 1, 2, and 3. The subscripts refer to the corresponding critical points on the frame.

The numbers m_k^+ and m_k^- can all be determined as linear functions of ϕ by solving the elastic frame, and the numbers $\bar{m}_k$ represent unknowns which are subject to the equilibrium equations with zero loads. The number ϕ_s will be the largest value of ϕ for which this problem possesses a solution. Although this is a well-defined problem in linear programming, we can solve it more simply by finding ϕ_{alt} and ϕ_{inc} and using (2.4.1).

It can be seen that the frame will not suffer from alternating plastic collapse provided the difference between the maximum and minimum elastic moments is less than twice the elastic range, i.e.,

$$M^+(s) - M^-(s) \le 2M_0 \tag{2.4.5}$$

For our example, in dimensionless quantities this can be written

$$m_k^+ - m_k^- \le 2 \tag{2.4.6}$$

which is easily solved for ϕ_{alt}.

To find ϕ_{inc} we use the fact that the frame must collapse in one of a finite number of mechanism modes, find the ϕ corresponding to each mode, and take ϕ_{inc} as the smallest of these numbers.

We illustrate these techniques for the frame in Fig. 4 and the values $f_1^* = 5$, $f_2^* = 0.4$. Then (2.2.1) becomes

$$0 \le f_1 \le 5\phi \qquad -0.4\phi \le f_2 \le 0.4\phi \tag{2.4.7}$$

We first solve the elastic problem and obtain Eqs. (2.1.6). Since these equations are linear and the load domain is convex, all $m_k^{\pm}$ must occur at vertices of the load domain - but not necessarily all at the same vertex.

The easiest way to find the vertex solutions is to take each load in turn equal to its maximum or minimum value while setting the other load equal to zero.

Putting $f_1 = 5\phi$, $f_2 = 0$ in Eq. (2.1.6) yields

$$\begin{aligned} m_1^e &= -0.234\phi \\ m_2^e &= 1.640\phi \\ m_3^e &= -0.234\phi \end{aligned} \tag{2.4.8}$$

Similarly $f_1 = 0$, $f_2 = \pm 0.4\phi$ yields

$$\begin{aligned} m_1^e &= \pm 0.2\phi \\ m_2^e &= \mp 0.1\phi \\ m_3^e &= \mp 0.2\phi \end{aligned} \tag{2.4.9}$$

Since the principle of superposition holds we can easily determine m^+ and m^- from Eqs. (2.4.8) and (2.4.9). The result is

$$\begin{aligned} m_1^+ &= 0.2\phi \qquad m_2^+ = 1.74\phi \qquad m_3^+ = 0.2\phi \\ m_1^- &= -0.434\phi \qquad m_2^- = -0.1\phi \qquad m_3^- = -0.434\phi \end{aligned} \tag{2.4.10}$$

The difference $m^+ - m^-$ at each of the points numbered 1, 2, and 3 is then

$$m_1^+ - m_1^- = 0.634\phi \qquad m_2^+ - m_2^- = 1.84\phi \qquad m_3^+ - m_3^- = 0.634\phi \tag{2.4.11}$$

We can prevent alternating plastic collapse by demanding that the elastic moment differences all satisfy (2.4.6). This implies

$$0.634\phi \le 2 \tag{2.4.12}$$

and therefore ϕ_{alt} is

$$\phi_{alt} = 3.155 \tag{2.4.13}$$

It remains to determine ϕ_{inc}. This value ϕ_{inc} can be most easily determined by observing that even though the frame is deformed gradually over many cycles, nevertheless the resulting deformed shape will be the same as that of a collapse mechanism. Suppose first that incremental collapse occurs in the collapse mechanism shown in Fig. 2(d). If the value ϕ_d is just sufficient to cause incremental collapse in mode (2d), at some stage of the loading process hinges must form at the points 2 and 3 in the sense indicated. Therefore the appropriate inequalities (2.4.4b) hold as equalities. This yields

$$\bar{m}_2 + m_2^+ = +1 \qquad \bar{m}_3 + m_3^- = -1 \tag{2.4.14}$$

Solving for $\bar{m}_2$, $\bar{m}_3$ and using Eqs. (2.4.10) we obtain

$$\bar{m}_2 = 1 - 1.74\phi \qquad \bar{m}_3 = -1 + 0.434\phi \tag{2.4.15}$$

The internal work due to these residual moments is

$$W_{INT} = (1-1.74\phi)(\theta+3\theta) + (-1+0.434\phi)(-\theta-3\theta) = 4\theta(2-2.174\phi) \tag{2.4.16}$$

But the external work is zero because the residual moments are in equilibrium with zero load. Therefore by the principle of virtual work, the internal work vanishes. Eq. (2.4.16) gives

$$\phi_d = 0.920 \tag{2.4.17d}$$

In a similar manner ϕ_{inc} corresponding to each of the other four collapse mechanisms may be found. The results are

$$\phi_b = 3.153 \tag{2.4.17b}$$

$$\phi_a = 0.920 \tag{2.4.17a}$$

$$\phi_c = 3.153 \tag{2.4.17c}$$

$$\phi_e = 0.676 \tag{2.4.17e}$$

corresponding to the collapse mechanisms in Figs. 2b, 2a, 2c, and 2e respectively. (Since $f_1 \geq 0$ it is not necessary to consider the other mechanisms). The smallest incremental collapse load is

$$\phi_{inc} = 0.676 \tag{2.4.18}$$

corresponding to Fig. (2e).

Comparing ϕ_{inc} to ϕ_{alt} we see that ϕ_{inc} is the smaller. This smallest value of ϕ is the shakedown factor ϕ_s given by

$$\phi_s = 0.676 \tag{2.4.19}$$

Therefore the loads f_1 and f_2 may vary arbitrarily within the bounds

$$0 \leq f_1 \leq 3.38 \qquad -0.27 \leq f_2 \leq 0.27 \tag{2.4.20}$$

and the frame will not collapse.

By way of comparison, the elastic multiplier ϕ_e is the largest multiplier such that no plastic behavior will occur for any load in the $D\phi_e$. It is easily found by computing the moments at the vertex loads and setting the numerically largest moment equal to its yield value. Thus, from Eqs. (2.1.6) with $f_1=5\phi$, $f_2=-0.4\phi$ we find

$$m_2 = 1.640\phi + 0.1\phi \leq 1 \tag{2.4.21}$$

hence

$$\phi_e = 1/1.740 = 0.575 \tag{2.4.22}$$

Therefore, in this example, shakedown analysis shows that the elastic analysis is overly conservative by about 15%.

On the other hand, the instantaneous collapse multiplier ϕ_{coll} is found by trying the various vertex loads in the mechanisms of Fig. 2. It is easy to see that when $f_1=5\phi$, $f_2=-0.4\phi$, mechanism e leads to a collapse load

$$\phi_{coll} = 8/7.9 = 1.013 \tag{2.4.23}$$

Therefore, if repeated loads are to be allowed, the instantaneous collapse load overestimates the true capacity by almost 50%.

3.1 Example of a frame acted upon by both a concentrated and a distributed load.

We look at the same pin-supported frame considered in section 2.1 with the exception that the concentrated load F_1 is now replaced by a distributed load as shown in Fig. 5. We will show that this frame can fail due to instantaneous, incremental or alternating plastic collapse as was the case for the frame loaded only by concentrated forces. However, the presence of the distributed load will cause this example to exhibit one further type of collapse behavior which we will call continuous plastic collapse.

We wish to determine the load domain for instantaneous plastic collapse. Consider the collapse mechanism for beam failure only shown in Fig. 6(a). It is assumed that the hinge lying between points C and D forms at a distance x from the point B where $x > 1$. According to Fig. 6(a) internal work is done at each of the three hinges, the total internal work W_{INT} is

$$W_{INT} = \theta + \theta + \frac{\theta x}{2-x} + \frac{\theta x}{2-x} = \frac{4}{2-x}\,\theta \qquad (3.1.1)$$

The external work W_{EXT} done by the loads f_1 and f_2 is given by

$$W_{EXT} = \int_1^x \left(\int_0^{t\theta} f_1 dy \right) dt + \int_x^2 \left(\int_0^{(2-t)\left(\frac{x\theta}{2-x}\right)} f_1 dy \right) dt \qquad (3.1.2)$$

which yields

$$W_{EXT} = (x-1/2) f_1 \theta \qquad (3.1.3)$$

The principle of virtual work implies

$$W_{INT} = W_{EXT} \tag{3.1.4}$$

which from Eqs. (3.1.1) and (3.1.3) results in

$$f_1 = \frac{8}{(2-x)(2x-1)} \tag{3.1.5}$$

The smallest value for the load f_1 is obtained when the hinge occurs at x=1.25, this value

$$f_1 = 7.111 \tag{3.1.6a}$$

is then the collapse load for the mechanism shown in Fig. 6(a).

In a similar manner we find that for each of the collapse mechanisms shown in Fig. 6(b), 6(c), 6(d), 6(e), 6(f), 6(g), the loads must satisfy

$$f_2 = 2 \tag{3.1.6b}$$

$$f_2 = -2 \tag{3.1.6c}$$

$$(x-1/2)f_1 + f_2 = \frac{4}{2-x} \tag{3.1.6d}$$

$$\left(x-\frac{5}{2}+\frac{1}{x}\right)f_1 + f_2 = -\frac{4}{x} \tag{3.1.6e}$$

$$f_1 = -7.111 \tag{3.1.6f}$$

$$\left(x-\frac{5}{2}+\frac{1}{x}\right)f_1 + f_2 = \frac{4}{x} \tag{3.1.6g}$$

$$(x-1/2)f_1 + f_2 = \frac{4}{x-2} \tag{3.1.6h}$$

respectively. We must examine Eqs. (3.1.6d,e,g,h) more closely before the location of the boundary for the load domain can be

determined. As an example we wi' . treat Eq. (3.1.6d). For a fixed value of f_1 the hinge position x which minimizes f_2 satisfies

$$\frac{4}{(2-x)^2} = f_1 \tag{3.1.7}$$

When this value for x and the fixed value for f_1 are substituted into Eq. (3.1.6d) we obtain the value of f_2 required for collapse. Thus the boundary may be obtained by choosing a value for either f_1 or x and then finding the corresponding f_2 by means of Eqs. (3.1.6d) and (3.1.7). Some results obtained from Eq. (3.1.6d) by the method are given in Table 6. In a similar way the boundaries represented by Eqs. (3.1.6e,g,h) may be found. The resulting load domain is shown in Fig. 7. In contrast to Fig. 3, this domain has curved sides. However, in both examples the load domain is convex.

In order to carry out a complete analysis of the frame for any given loading program we must find the equations which govern any stage of that loading program. Consider the free-body diagram shown in Fig. 8. We can show that the moments along the frame are given in terms of a single redundant H by

$$\begin{aligned} M_{AB} &= -Hy & 0 \le y \le 1 \\ M_{BC} &= -H + (1/4F_1-1/2F_2)x & 0 \le x \le 1 \\ M_{CD} &= -H + (1/4F_1-1/2F_2)x - 1/2f_1(x-1)^2 & 1 \le x \le 2 \\ M_{DE} &= -(H+f_2)y & 0 \le y \le 1 \end{aligned} \tag{3.1.8}$$

f_1	x, position of hinge	f_2
7.111	1.250	0
6.5	1.216	0.448
6.0	1.184	0.798
5.5	1.147	1.131
5.0	1.106	1.444
4.5	0.939	1.795
4.0	1	2

Table 6

Load Domain and Hinge Locations

for Frame of Fig. 6

where M_{AB} is the moment along the frame between the points A and B and similarly for M_{BC}, M_{CD}, and M_{DE}.

The elastic energy for the frame may be determined by means of Eqs. (3.1.8). When the elastic energy is minimized with respect to the redundant H, we find

$$H = 1/8f_1 - 1/2f_2 \tag{3.1.9}$$

and hence obtain the elastic solution

$$\begin{aligned} M_{AB} &= -(1/8f_1-1/2f_2)y \\ M_{BC} &= -1/8f_1 + 1/2f_2 + (1/4f_1-1/2f_2)x \\ M_{CD} &= -1/8f_1 + 1/2f_2 + (1/4f_1-1/2f_2)x - 1/2f_1(x-1)^2 \\ M_{DE} &= -(1/8f_1+1/2f_2)y \end{aligned} \tag{3.1.10}$$

The moment is piecewise linear except in CD where it is quadratic, provided $f_1 \neq 0$. Formally setting the derivative of M_{CD} equal to zero yields

$$x_m = 5/4 - f_2/(2f_1) \tag{3.1.11a}$$

which will lie between 1 and 2 (i.e., be on CD)

$$\begin{aligned} &\text{IF } (f_1 > 0 \quad \text{AND} \quad -3f_1 < 2f_2 < f_1) \\ &\text{OR } (f_1 < 0 \quad \text{AND} \quad f_1 < 2f_2 < -3f_1) \end{aligned} \tag{3.1.11b}$$

Thus we may limit our analysis to a consideration of the moments at the points B, C, D, and x_m. We are now in a position to investigate specific loading paths which result in collapse of the frame.

3.2 Instantaneous plastic collapse.

We set $f_2=0$ in the elastic solution, Eqs. (3.1.10), and increase f_1 from zero. We find that the elastic solution holds until

$$f_1 = \frac{32}{5} = 6.4 \qquad (3.2.1)$$

at which point the moment reaches positive yield at x=5/4. At this stage the moments are

$$M_{BC} = -0.8 + 1.6x$$
$$M_{CD} = -0.8 + 1.6x - 3.2(x-1)^2 \qquad (3.2.2)$$

We continue to increase f_1 while regarding the frame as an elastic structure with a perfect hinge at x=1.25 acted upon by the additional load. As before the quantities in the auxiliary problem will be denoted by bars. Equations (3.1.8) govern the solution during this stage. We set

$$\bar{M}_{CD}\,(1.25) = 0 \qquad (3.2.2)$$

which implies

$$\bar{M} = \frac{9}{32}\,\bar{f}_1 \qquad (3.2.3)$$

and thus the changes in the moments are given by

$$\bar{M}_{BC} = -\frac{9}{32}\,\bar{f}_1 + 1/4\bar{f}_1 x$$
$$M_{CD} = -\frac{9}{32}\,\bar{f}_1 + 1/4\bar{f}_1 x - 1/2\bar{f}_1(x-1)^2 \qquad (3.2.4)$$

We terminate this stage when $\bar{f}_1=0.4$. At this point, we have

$$\bar{M}_{BC} = -0.113 + 0.1x$$
$$\bar{M}_{CD} = -0.113 + 0.1x - 0.2(x-1)^2 \qquad (3.2.5)$$

Eqs. (3.2.2) and (3.2.5) give the complete solution for $f_1=6.8$

$$M_{BC} = -0.913 + 1.7x$$
$$M_{CD} = -0.913 + 1.7x - 3.4(x-1)^2 \qquad (3.2.6)$$

For the next stage of this loading program we hold $f_1=6.8$ and we increase f_2. The elastic equations (3.1.10) show that an increase in f_2 will decrease the moment at x=1.25. Therefore, the frame will be fully elastic during this stage and is governed by Eqs. (3.1.10). The auxiliary solution is

$$\bar{f}_1 = 0$$
$$\bar{M}_{BC} = 1/2\bar{f}_2 - 1/2\bar{f}_2 x = \bar{M}_{CD} \qquad (3.2.7)$$

Therefore, the complete solution is

$$f_1 = 6.8 \qquad f_2 = \bar{f}_2$$
$$M_{BC} = -0.913 + 1/2\bar{f}_2 + (1.7-1/2\bar{f}_2)x \qquad (3.2.8)$$
$$M_{CD} = -0.913 + 1/2\bar{f}_2 + (1.7-1/2\bar{f}_2)x - 3.4(x-1)^2$$

This solution is valid until $\bar{f}_1=0.175$ at which value M_{CD} reaches negative yield at x=2, i.e., at the point D. The solution is

$$f_1 = 6.8 \qquad f_2 = 0.175$$
$$M_{BC} = -0.826 + 1.613x \qquad (3.2.9)$$
$$M_{CD} = -0.826 + 1.613x - 3.4(x-1)^2$$

We continue to increase f_2 but this time we consider an auxiliary problem with a perfect hinge at the point D. The auxiliary solution is

$$\bar{f} = 0, \qquad \bar{M}_{BC} = \bar{M}_{CD} = \bar{f}_2 - 1/2\bar{f}_2 x \qquad (3.2.10)$$

The complete solution is

$$f_1 = 6.8 \qquad f_2 = 0.175 + \bar{f}_2$$

$$M_{BC} = -0.826 + \bar{f}_2 + (1.613 - 1/2\bar{f}_2)x \tag{3.2.11}$$

$$M_{CD} = -0.826 + \bar{f}_2 + (1.613 - 1/2\bar{f}_2)x - 3.4(x-1)^2$$

This solution is valid until $\bar{f}_2 = 0.056$ at which point there is a positive yield moment at $x = 1.233$. The frame is now in the collapse mechanism shown in Fig. 6(d). The complete solution at this point of instantaneous plastic collapse is given by

$$f_1 = 6.8 \qquad f_2 = 0.231$$

$$M_{BC} = -0.77 + 1.585x \tag{3.2.12}$$

$$M_{CD} = -0.77 + 1.585x - 3.4(x-1)^2$$

This loading program is summarized in Table 7. The loading path is OAB as illustrated in Fig. 7.

3.3 Incremental plastic collapse.

The initial stages of the loading program for incremental plastic collapse are the same as those for instantaneous plastic collapse in the previous section. Table 7 holds up through stage 4U, i.e., we have $f_1 = 6.8$ and are increasing f_2 from 0.175. We stop increasing f_2 at the value $f_2 = 0.2$ and the complete solution is then given by Eq. (3.2.11) with $\bar{f}_2 = 0.025$, i.e.,

Stage	Control	Moments	f_1	f_2	M_{BC}	M_{CD}	Terminate
1U	f_1	all elastic	1	0	$-1/8+1/4x$	$-1/8+1/4x-1/2(x-1)^2$	
1L			6.4	0	$-0.8+1.6x$	$-0.8+1.6x-3.2(x-1)^2$	P^+ at $x=1.25$
2U	$+\Delta f_1$	P^+ at $x=1.25$	1	0	$-9/32+1/4x$	$-9/32+1/4x-1/2(x-1)^2$	
2Δ			0.4	0	$-0.113+0.1x$	$-0.113+0.1x-0.2(x-1)^2$	
2L			6.8	0	$-0.913+1.7x$	$-0.913+1.7x-3.4(x-1)^2$	$f_1=6.8$
3U	$+\bar{f}_2$	all elastic	0	1	$1/2-1/2x$	$1/2-1/2x$	
3Δ			0	0.175	$0.088-0.088x$	$0.088-0.088x$	
3L			6.8	0.175	$-0.826+1.613x$	$-0.826+1.613x-3.4(x-1)^2$	P^- at $x=2$
4U	$+\Delta f_2$	P^- at $x=2$	0	1	$1-1/2x$	$1-1/2x$	
4Δ			0	0.056	$1-0.028x$	$1-0.028x$	
4L			6.8	0.231	$-0.77+1.585x$	$-0.77+1.585x-3.4(x-1)^2$	P^+ at $x=1.233$

Table 7

Complete History Illustrating Instantaneous Plastic Collapse with Distributed Load

$$f_1 = 6.8 \qquad f_2 = 0.2$$

$$M_{BC} = -0.8 + 1.6\,x \tag{3.3.1}$$

$$M_{CD} = -0.8 + 1.6\,x - 3.4(x-1)^2$$

We now decrease f_1. Eqs. (3.1.10) show that a decrease in f_1 will result in an increase in the moment at the point x=2 and thus the frame returns to fully elastic behavior. The auxiliary solution is

$$\bar{M}_{BC} = -1/8\bar{f}_1 + 1/4\bar{f}_1 x \tag{3.3.2}$$

$$\bar{M}_{CD} = -1/8\bar{f}_1 + 1/4\bar{f}_1 x - 1/2\bar{f}_1(x-1)^2$$

The complete solution is then

$$f_1 = 6.8 + \bar{f}_1 \qquad f_2 = 0.2$$

$$M_{BC} = -0.8 - 1/8\bar{f}_1 + (1.6 + 1/4\bar{f}_1)x \tag{3.3.3}$$

$$M_{CD} = -0.8 - 1/8\bar{f}_1 + (1.6 + 1/4\bar{f}_1)x - (3.4 + 1/2\bar{f}_1)(x-1)^2$$

We choose to stop decreasing f_1 when it reaches the value f_1=6.72. We note that an examination of Eqs. (3.3.3) at the initial points B, C, D, and

$$x = 5/4 - 1/2\left(\frac{0.2}{\bar{f}_1}\right) \tag{3.3.4}$$

will show that no yielding takes place during this unloading. The complete solution for f_1=6.72, f_2=0.2 is

$$M_{BC} = -0.79 + 1.58x \tag{3.3.5}$$

$$M_{CD} = -0.79 + 1.58x - 3.36(x-1)^2$$

The next stage involves decreasing f_2 and again the elastic equations (3.1.10) govern the solution. During this stage the solution is

$$f_1 = 6.72 \qquad f_2 = 0.2 + \bar{f}_2$$

$$M_{BC} = -0.79 + 1/2\bar{f}_2 + (1.58 - 1/2\bar{f}_2)x \tag{3.3.6}$$

$$M_{CD} = -0.79 + 1/2\bar{f}_2 + (1.58 - 1/2\bar{f}_2)x - 3.36(x-1)^2$$

By considering the critical points B, C, D, and

$$x = 5/4 - 1/2\,\frac{f_2}{6.72} \tag{3.3.7}$$

we can show that no yielding occurs during this unloading until f_2=0 at which value there is a positive yield hinge at x=1.25. The complete solution is

$$f_1 = 6.72 \qquad f_2 = 0$$

$$M_{BC} = -0.89 + 1.68x \tag{3.3.8}$$

$$M_{CD} = -0.89 + 1.68x - 3.36(x-1)^2$$

We now increase f_1. During this loading the hinge with positive yield moment will remain at x=1.25. The solution is

$$f_1 = 6.72 + \bar{f}_1 \qquad f_2 = 0$$

$$M_{BC} = -0.89 - 9/32\bar{f}_1 + (1.68 + 1/4\bar{f}_1)x \tag{3.3.9}$$

$$M_{CD} = -0.89 - 9/32\bar{f}_1 + (1.68 + 1/4\bar{f}_1)x - (3.36 + 1/2\bar{f}_1)(x-1)^2$$

No further yielding occurs as f_1 is increased to 6.8, the solution at this point being

Table 8

Complete History Illustrating Incremental

Plastic Collapse with Distributed Load

Stage	Control	Moments	f_1	f_2	m_{BC}	m_{CD}	Terminate
1L			6.4	0	$-0.8+1.6x$	$-0.8+1.6x-3.2(x-1)^2$	P^+at $x=1.25$
2L			6.8	0	$-0.913+1.7x$	$-0.913+1.7x-3.4(x-1)^2$	$f_1=6.8$
3L			6.8	0.175	$-0.826+1.613x$	$-0.826+1.613x-3.4(x-1)^2$	P^-at $x=2$
4U	$+\Delta f_2$	P^-at $x=2$	0	1	$1-1/2x$	$1-1/2x$	
4Δ			0	0.025	$0.025-0.013x$	$0.025-0.013x$	
4L			6.8	0.2	$-0.8+1.6x$	$-0.8+1.6x-3.4(x-1)^2$	$f_2=0.2$
5U	$-\Delta f_1$	all elastic	-1	0	$1/8-1/4x$	$1/8-1/4x+1/2(x-1)^2$	
5Δ			0.08	0	$0.01-0.02x$	$0.01-0.02x+0.04(x-1)^2$	
5L			6.72	0.2	$-0.79+1.58x$	$-0.79+1.58x-3.36(x-1)^2$	$f_1=6.72$
6U	$-\Delta f_2$	all elastic	0	-1	$-1/2+1/2x$	$-1/2+1/2x$	
6Δ			0	0.2	$-0.1+0.1x$	$-0.1+0.1x$	
6L			6.72	0	$-0.89+1.68x$	$-0.89+1.68x-3.36(x-1)^2$	P^+at $x=1.25$
7U	$+\Delta f_1$	P^+at $x=1.25$	1	0	$-9/32+1/4x$	$-9/32+1/4x-1/2(x-1)^2$	
7Δ			0.08	0	$0.023+0.02x$	$0.023+0.02x-0.04(x-1)^2$	
7L			6.8	0	$-0.913+1.7x$	$-0.913+1.7x-3.4(x-1)^2$	$f_1=6.8$

$$f_1 = 6.8 \qquad f_2 = 0$$

$$M_{BC} = -0.913 + 1.7x \tag{3.3.10}$$

$$M_{CD} = -0.913 + 1.7x - 3.4(x-1)^2$$

This solution is the same as that obtained for stage 2L as shown in Table 8. Therefore, we have in fact completed a cycle and stages 3 to 7 will be repeated each time the load point traverses ACDEA in Fig. 7. By the same argument as that in section 2.1.b we can see that after a finite number of cycles the frame will fail in the collapse mechanism shown in Fig. 6(d).

3.4 Alternating plastic collapse.

Alternating plastic collapse can be brought about by following the loading path OAFAF... as shown in Fig. 7. The load f_1 is increased to 6.8 which is the point B in Fig. 7 and then decreased below zero to -6.4, i.e., to the point G, finally f_1 is increased to 6.8 again. The results are summarized in Table 9. By the same argument that we used in section 2.1.c we can see that after a finite number of cycles a frame made of any real material will fail at the point x=1.25.

3.5 Continuous plastic collapse.

We now consider the fourth type of collapse behavior, namely continuous plastic collapse which may happen when a distributed load acts on our simple frame. The loading path is given by OACAC... and is the same as that for incremental collapse up through stage 4L given in Table 8. However, for this example the fifth stage consists of decreasing f_2 to 0.102 at which point a hinge with positive yield moment forms at x=1.243. The complete solution for f_1=6.8, f_2=0.102 is

Table 9

Complete History Illustrating Alternating Plastic Collapse with Distributed Load

Stage	Control	Moments	f_1	f_2	M_{BC}	M_{CD}	Terminate
1L	f_1	all elastic	6.4	0	-0.8+1.6x	-0.8+1.6x-3.2(x-1)^2	P^+ at x=1.25
2L	$+\Delta f_1$	P^+ at x=1.25	6.8	0	-0.913+1.7x	-0.913+1.7x-3.4(x-1)^2	f_1=6.8
3U	$-\Delta f_1$	all elastic	-1	0	1/8-1/4x	1/8-1/4x+1/2(x-1)^2	
3Δ			12.8	0	1.6-3.2x	1.6-3.2x+6.4(x-1)^2	
3L			-6.0	0	0.687-1.5x	0.687-1.5x+3(x-1)^2	P^- at x=1.25
4U	$-f_1$	P^- at x=1.25	-1	0	9/32-1/4x	9/32-1/4x+1/2(x-1)^2	
4Δ			0.4	0	0.113-0.1x	0.113-0.1x+0.2(x-1)^2	
4L			-6.4	0	0.8-1.6x	0.8-1.6x+3.2(x-1)^2	f_1=-6.4
5U	$+\Delta f_1$	all elastic	1	0	-1/8+1/4x	-1/8+1/4x-1/2(x-1)^2	
5Δ			12.8	0	-1.6+3.2x	-1.6+3.2x-6.4(x-1)^2	
5L			6.4	0	-0.8+1.6x	-0.8+1.6x-3.2(x-1)^2	P^+ at x=1.25

$$M_{BC} = -0.849 + 1.649x$$
$$M_{CD} = -0.849 + 1.649x - 3.4(x-1)^2 \qquad (3.5.1)$$

We now decrease f_2 further. If we assume that the hinge remains at x=1.243 we find that Eqs. (3.1.8) give moments whose magnitude is greater than unity which is inconsistent. Therefore, we assume that as f_2 decreases the hinge changes position. Eqs. (3.1.8) govern the solution of the auxiliary problem and yield

$$\bar{M}_{BC} = -\bar{H} - 1/2\bar{f}_2 x = \bar{M}_{CD} \qquad (3.5.2)$$

We combine Eqs. (3.5.1) and (3.5.2) to obtain the complete solution

$$f_1 = 6.8 \qquad f_2 = 0.102 + \bar{f}_2 \qquad \bar{f}_2 \leq 0$$
$$M_{BC} = -0.849 - \bar{H} + (1.649-1/2\bar{f}_2)x \qquad (3.5.3)$$
$$M_{CD} = -0.849 - \bar{H} + (1.649-1/2\bar{f}_2)x - 3.4(x-1)^2$$

We now note that at the point at which a hinge forms the moment is an extremum. From Eq. (3.5.3) M_{CD} is a maximum at the point

$$x = 1.243 - 1/2\,\frac{\bar{f}_2}{6.8} \qquad (3.5.4)$$

and hence we impose the condition that the moment be equal to unity at the point x given by Eq. (3.5.4). This condition gives

$$\bar{H} = -0.621\bar{f}_2 + 0.018(\bar{f}_2)^2 \qquad (3.5.5)$$

By means of Eq. (3.5.5) $\bar{H}$ may be eliminated from Eq. (3.5.3) to yield

$$M_{BC} = -0.849 + 0.621\bar{f}_2 - 0.018(\bar{f}_2)^2 + (1.649-1/2\bar{f}_2)x \qquad (3.5.6)$$
$$M_{CD} = -0.849 + 0.621\bar{f}_2 - 0.018(\bar{f}_2)^2 + (1.649-1/2\bar{f}_2)x - 3.4(x-1)^2$$

It should be noted that during this unloading there is always a hinge present with positive yield moment whose position is given by Eq. (3.5.4). On examining Eqs. (3.5.6) for the points B, C, and D we can show that no yielding occurs at these points as f_2 is reduced to zero. At $f_2=0$ the complete solution is

$$f_1 = 6.8 \qquad f_2 = 0$$

$$M_{BC} = -0.913 + 1.7x \tag{3.5.7}$$

$$M_{CD} = -0.913 + 1.7x - 3.4(x-1)^2$$

at which point the hinge is at x=1.25. These results are summarized in Table 10. Since row 6L is identical to row 2L we have in fact completed a cycle. During each cycle the same work will be done and since a real material can absorb only a finite amount of work, it is clear that the frame will collapse after some finite number of cycles.

Each cycle will produce a slope discontinuity at D as f_2 is increased from 0.175 to 0.2, so that after a large number of cycles there will be a large discontinuity of slope at D. However, as f_2 is decreased from 0.102 to 0.0 in each cycle, the hinge on the beam will move continuously from x=1.243 to x=1.25. After a large number of cycles there will be a large difference in the slopes at x=1.243 and x=1.25, but the slope between those two points will always vary continuously. Therefore, although the deformations can become indefinitely large, the deformed shape will not correspond to any one of the mechanisms in Fig. 6.

3.6 Shakedown behavior.

Clearly there will also exist loading cycles which produce totally elastic behavior and limited plastic behavior as discussed in Secs. 2.1.d and 2.1.e for concentrated loads. We do not detail any results.

Stage	Control	Moments	f_1	f_2	M_{BC}	M_{CD}	Terminate
1L	f_1	all elastic	6.4	0	$-0.8+1.6x$	$-0.8+1.6x-3.2(x-1)^2$	P^+ at x=1.25
2L	$+\Delta f_1$	P^+ at x=1.25	6.8	0	$-0.913+1.7x$	$-0.913+1.7x-3.4(x-1)^2$	$f_1=6.8$
3L	$+f_2$	all elastic	6.8	0.175	$-0.826+1.613x$	$-0.826+1.613x-3.4(x-1)^2$	P^- at x=2
4L	$+\Delta f_2$	P^- at x=2	6.8	0.2	$-0.8+1.6x$	$-0.8+1.6x-3.4(x-1)^2$	$f_2=0.2$
5U	$-\Delta f_2$	all elastic	0	-1	$-1/2\Delta f_2+1/2\Delta f_2 x$	$-1/2\Delta f_2+1/2\Delta f_2 x$	
5L			6.8	0.102	$-0.849+1.649x$	$-0.849+1.649x-3.4(x-1)^2$	P^+ at x=1.243
6U	$-\Delta f_2$	P^+ at x=1.243 $+1/2\,\frac{\Delta f_2}{6.8}$	0	-1	$-0.621\Delta f_2-0.118(\Delta f_2)^2$ $-1/2(\Delta f_2)x$	$-0.621\Delta f_2-0.118(\Delta f_2)^2$ $-1/2(\Delta f_2)x$	
6L			6.8	0	$-0.913+1.7x$	$-0.913+1.7x-3.4(x-1)^2$	$f_2=0$

Table 10

Complete History Illustrating Continuous Plastic Collapse with Distributed Load.

3.7 Collapse domain for frame under distributed loads.

We can see from the foregoing examples that the presence of a distributed load acting on the frame introduces a fourth type of collapse behavior, continuous plastic collapse, in addition to instantaneous, incremental, and alternating plastic collapse. Clearly, the definition of a collapse domain given in Section 2.2 must be modified to take account of this fourth type of collapse behavior. As in the original definition, we consider any load path in a domain D defined by the inequalities

$$-f_1^* \le f_1 \le f_1^* \qquad -f_2^* \le f_2 \le f_2^* \tag{3.7.1}$$

where f_1^* and f_2^* are assigned extreme magnitudes for the loads f_1 and f_2 respectively.

The modified definition is: i) If any load cycle results in instantaneous, incremental, alternating, or continuous plastic collapse, then D is a collapse domain, ii) If all load cycles eventually result in fully elastic behavior, possibly after some initial plastic flow, then D is a shakedown domain.

3.8 Shakedown multiplier.

As in the case of a frame under concentrated loads we can define a field G of load domains by requiring that the loads satisfy the inequalities

$$\phi f_1^* \le f_1 \le \phi f_1^* \qquad -\phi f_2^* \le f_2 \le \phi f_2^* \tag{3.8.1}$$

D_ϕ denotes the load domain corresponding to a particular value for ϕ in the inequalities (3.8.1).

The shakedown multiplier ϕ_s is defined in terms of the modified definitions of collapse and shakedown domains given above. ϕ_s has the properties: i) for any $\phi \le \phi_s$, D_ϕ is a shakedown domain and ii) for any $\phi > \phi_s$, D_ϕ is a collapse domain.

The shakedown problem is still defined by Eqs. (2.4.4a) but Eqs. (2.4.4b) are no longer adequate. As we shall demonstrate, it is possible to extend the methods of the previous section and find ϕ_{alt} and ϕ_{inc} in the case of distributed loads. However, it follows from our definition, that

$$\phi_s = \min(\phi_{inc}, \phi_{alt}, \phi_{con}) \tag{3.8.2}$$

where ϕ_{con} is defined as the smallest ϕ for which continuous plastic collapse can occur so that it is necessary that we either

(1) find ϕ_{con} or (3.8.3a)

(2) show that $\phi_{con} \ge \phi_{inc}$ (3.8.3b)

in order to establish ϕ_s.

3.9 Determination of the shakedown multiplier for a simple frame under distributed loads.

We return to the example of the frame under distributed loads shown in Fig. 5. For our example, the loads f_1 and f_2 are allowed to vary arbitrarily between the bounds

$$0 \le f_1 \le 6.8\phi \qquad 0 \le f_2 \le 0.2\phi \tag{3.9.1}$$

Recalling the discussion in Section 2.4, our first task is to determine $m^+(s)$ and $m^-(s)$, the maximum and minimum values respectively of the dimensionless elastic moment $m^e(s)$ at any point a distance s along the frame. The equations (3.1.10) for the elastic solution are given below.

$$M_{AB} = -(1/8f_1 - 1/2f_2)y$$

$$M_{BC} = -1/8f_1 + 1/2f_2 + (1/4f_1 - 1/2f_2)x \qquad (3.9.2)$$

$$M_{CD} = -1/8f_1 + 1/2f_2 + (1/4f_1 - 1/2f_2)x - 1/2f_1(x-1)^2$$

$$M_{DE} = -(1/8f_1 + 1/2f_2)y$$

Since M_{AB}, M_{DE} are linear in y and M_{BC} is linear in x we need only determine M^+ and M^- at the points B, C, and D and as a function of x for points between C and D.

The first step is to find the elastic moments corresponding to vertex points on the given domain from which M^+, M^- may be determined for any point on the frame by superposition. A trivial case is $f_1=0$ and $f_2=0$ in which case the moments are zero at any point on the frame. For $f_1=6.8\phi$ and $f_2=0$ we have

$$M_B = -0.85\phi \qquad M_C = 0.85\phi \qquad M_D = -0.85\phi$$

$$M_{CD} = [-0.85+1.7x-3.4(x-1)^2]\phi \qquad (3.9.3)$$

For $f_1=0$, $f_2=0.2\phi$ the solution is

$$M_B = 0.1\phi \qquad M_C = 0 \qquad M_D = -0.1\phi$$

$$M_{CD} = [0.1-0.1x]\phi \qquad (3.9.4)$$

Finally, by superposition of these solutions we obtain

$$M_B^+ = 0.1\phi \qquad M_B^- = -0.85\phi \qquad (3.9.5a)$$

$$M_C^+ = 0.85\phi \qquad M_C^- = 0 \qquad (3.9.5b)$$

$$M_D^+ = 0 \qquad M_D^- = -0.95\phi \qquad (3.9.5c)$$

$$M_{CD}^+ = \begin{cases} [-0.85+1.7x-3.4(x-1)^2]\phi & 1 \le x \le 1.809 \\ 0 & 1.809 \le x \le 2 \end{cases} \qquad (3.9.5d)$$

$$M_{CD}^- = \begin{cases} (0.1-0.1x)\phi & 1 \le x \le 1.809 \\ [-0.75+1.6x-3.4(x-1)^2]\phi & 1.809 \le x \le 2 \end{cases} \qquad (3.9.5d)$$

The differences between the maximum and minimum moments are then

$$\Delta_B \equiv M_B^+ - M_B^- = 0.95\phi \qquad (3.9.6a)$$

$$\Delta_C \equiv M_C^+ - M_C^- = 0.85\phi \qquad (3.9.6b)$$

$$\Delta_D \equiv M_D^+ - M_D^- = 0.95\phi \qquad (3.9.6c)$$

$$\Delta_x(x) = M_{CD}^+ - M_{CD}^- = \begin{cases} [-0.95+1.8x-3.4(x-1)^2]\phi & 1 \le x \le 1.809 \\ [0.75-1.6x+3.4(x-1)^2]\phi & 1.809 \le x \le 2 \end{cases} \qquad (3.9.6d)$$

From Eq (3.9.6d) we can show that $M_{CD}^+(x) - M_{CD}^-(x)$ attains its maximum value of 1.088ϕ at $x=1.265$, i.e.,

$$\Delta_{CD} \equiv \max_{1<x<2} \left[M_{CD}^+(x) - M_{CD}^-(x)\right] = 1.088\phi \qquad (3.9.7)$$

The condition that the frame will not suffer alternating plastic collapse is given by Eq. (2.4.5) which reduces in dimensionless form to

$$M^+(s) - M^-(s) \le 2 \qquad (3.9.8)$$

This condition must hold for all s but for our example it is necessary and sufficient to consider only the differences Δ_B, Δ_C, Δ_D, and Δ_{CD} given in Eqs. (3.9.6) and (3.9.7). Clearly the most stringent requirement is Δ_{CD}, whence

$$\phi_{alt} = 1.838 \qquad (3.9.9)$$

In the calculation of ϕ_{inc} there are three collapse mechanisms to be considered as shown in Figs. 6(a), 6(b), and 6(d). We will treat the mechanism shown in Fig. 6(d) in which there is

a hinge with positive yield moment present at a distance x from the point B and the hinge at the point D has a negative yield moment. Equations (2.4.4a) hold as equalities so that the residual moments satisfy

$$\bar{M}_D + M_D^- = -1 \qquad \bar{M}_{CD}(x) + M_{CD}^+(x) = 1 \tag{3.9.10}$$

for some $1 < x < 2$. We now set the internal work due to the residual moments equal to zero. This gives

$$\bar{M}_{CD}(x)[\theta + \frac{x}{2-x}\theta] + \bar{M}_D[-\theta - \frac{x}{2-x}\theta] = 0 \tag{3.9.11}$$

which reduces to

$$\bar{M}_{CD}(x) - \bar{M}_D = 0 \tag{3.9.12}$$

We now consider two cases;

Case i) $1 \leq x \leq 1.809$; By means of Eqs. (3.9.5) and (3.9.10), Eq. (3.9.12) may be written

$$1 + [0.85-1.7x+3.4(x-1)^2]\phi + 1 - 0.95\phi = 0 \tag{3.9.13}$$

which implies

$$\phi = \frac{2}{[0.1+1.7x-3.4(x-1)^2]} \tag{3.9.14}$$

The smallest value for ϕ occurs when x=1.25, this value being

$$\phi_d^{(i)} = 0.994 \tag{3.9.15}$$

where the subscript d refers to the type of collapse mechanism (in this case Fig. 6(d)) and the superscript (i) denotes the range of x from which $\phi_d^{(i)}$ was calculated.

Case ii) $1.809 \leq x \leq 2$; By means of equations (3.9.5) and (3.9.10) Eq. (3.9.12) becomes

$$1 + 1 - 0.95\phi = 0 \tag{3.9.16}$$

which implies

$$\phi_d^{(ii)} = 2.105 \tag{3.9.17}$$

In a similar way we determine

$$\phi_a^{(i)} = 1.013$$

$$\phi_a^{(ii)} = 2.105 \tag{3.9.18}$$

$$\phi_b = 2.105$$

Therefore

$$\phi_{inc} = 0.944 \tag{3.9.19}$$

We assume for the moment that ϕ_s is the smaller of ϕ_{inc} and ϕ_{alt}, i.e., that

$$\phi_s = 0.994 \tag{3.9.20a}$$

The associated residual moment field is defined by

$$\bar{M}_B = \bar{M}_D = \bar{M}_{CD}(x) = -0.056 \tag{3.9.20b}$$

for all points on the top span of the frame. It then follows from (3.9.5) and (3.9.20) that the moments must satisfy

$$\begin{aligned} &-0.901 \leq M_B \leq 0.043 \\ &-1 \leq M_D \leq -0.056 \\ &.043-.099x \leq M_{CD}(x) \leq 1-3.379(x-5/4)^2 \qquad 1 \leq x \leq 1.809 \\ &-1+.199(2-x)(17x-8) \leq M_{CD}(x) \leq -0.056 \qquad 1.809 \leq x \leq 2 \end{aligned} \tag{3.9.21}$$

for all load points in D_{ϕ_s}. Clearly the only yield moments which can be reached are

$$M_{CD}(5/4) = +1 \qquad M_{CD}(2) \equiv M_D = -1 \qquad (3.9.22)$$

so that no form of continuous collapse is possible. Thus, for this example, (3.8.3b) holds and we can find ϕ_s without considering the possibility of continuous collapse.

4. Future research

For the simple example considered in Sec. 3 we have shown

(1) *The shakedown multiplier can be determined from*

$$\phi_s = \min(\phi_{inc}, \phi_{alt}) \qquad (4.1)$$

(2) *There is no loading path in D_{ϕ_s} for which continuous collapse can occur.*

(3) *For a particular collapse domain a load path exists for which failure is caused by continuous collapse.*

Future research will be concerned first with the generality of these conclusions. We will attempt to either prove that they hold for all possible combinations of distributed loads or to find a counter example where conclusions (1) and/or (2) are invalid. If such a counter example is found for conclusion (1) we will then seek to determine limits on the validity of the conclusion and also to investigate simple means of determining ϕ_{con}.

In our discussion of the simple frame axial forces were neglected and we assumed that the yield strength of the material depended only on the bending moment. It is our intention in future work to investigate the effect of the inclusion of axial forces with regard to the determination of the shakedown domain.

The treatment of axial forces in frames and arches is discussed in Chapt. 7 of Ref. [1]. In order to give some idea as to our future work we consider a qualitative picture as shown in Fig. 9 of a typical interaction curve in the stress resultant plane corresponding to a structure whose cross-section is rectangular. In Fig. 9 m and n denote the dimensionless moment and dimensionless axial force respectively. When axial forces are neglected it is clear that yielding can occur only when the moment

at the position where the hinge will occur reaches the points A or B. However, when axial forces are included the hinge may form when the stress resultant (m,n) lies at any point along the interaction curve ABCD.

We see that it is possible to consider a hinge whose position is fixed but for which the corresponding stress resultant (m,n) may move along an arc AE, for example, of the interaction curve. Since the strain-rate vector $(\dot{\theta},\dot{e})$ must be normal to the interaction curve we see that it changes direction as the stress resultant (m,n) moves along the arc AE.

Thus when axial forces are included incremental plastic collapse might occur under a loading path for which a hinge forms at the same position on a given structure during each cycle but for which the strain rate vector has a different direction at yield during different parts of each such cycle. Therefore, when axial forces are considered we not only have the possibility of continuous collapse due to motion of the hinge along the structure, but we also have the possibility of what may be termed a complex-hinge collapse where the hinge location is fixed but the mechanism involves continuous variations in the ratio of rotation rate $\dot{\theta}$ to axial extension rate $\dot{e}$. Still further complications may be introduced by possible interactions between these two effects.

The concept of alternating collapse is also more complicated when axial forces are considered. Under bending only, alternating collapse is simply defined by the existence of any load cycle for which the moment-point at any specific location in the structure can be at points A and C in Fig. 9 for different load states in the cycle. Now, however, there is the additional possibility that

it be at points A and G, say. Such behavior would certainly be physically undersirable. Local analysis would show that part of the cross section would alternately yield in tension and compression, hence alternating collapse would be expected. However, suppose the cycle permitted both points A and E to occur repeatedly. Is this also a form of alternating collapse? If so, the simple techniques described in Sec. 3 are inadequate and must be generalized; if not, how far away must two points be to refer to the resulting failure as alternating collapse?

For these problems also, our general approach will be to first consider simple problems and look for counter examples, and then to consider more general structures and loadings and attempt to either prove the validity of (4.1) or to specify its limits and find its simplest generalization.

Reference.

1. P. G. Hodge, "Plastic Analysis of Structures", McGraw-Hill Co., 1959.

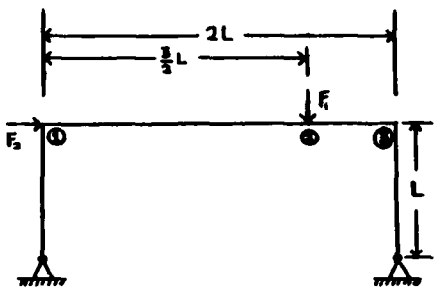

Fig. 1 Frame Under Concentrated Loads.

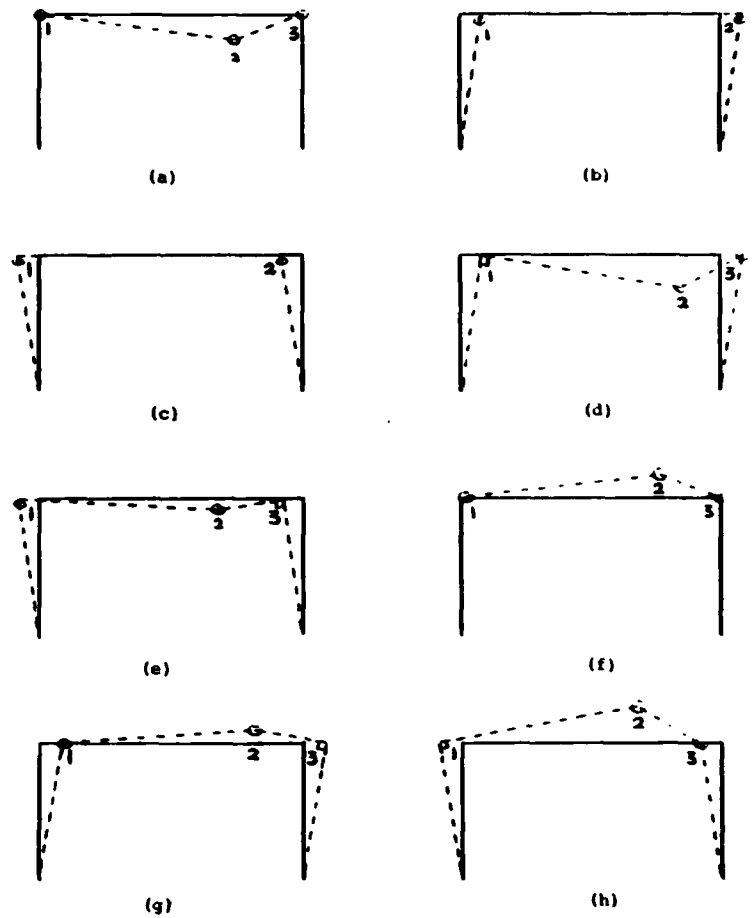

Fig. 2. Collapse Mechanisms for the Frame of Fig. 1.

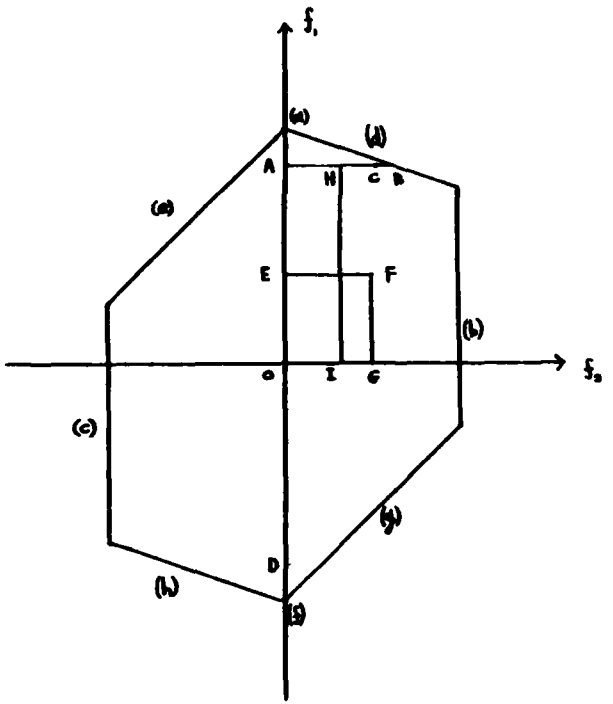

Fig. 3. Domain of Loads for the Frame of Fig. 1 for which Instantaneous Plastic Collapse Cannot Occur.

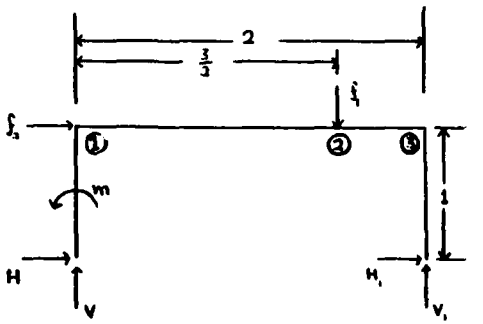

Fig. 4 Free-Body Diagram for the Frame of Fig. 1.

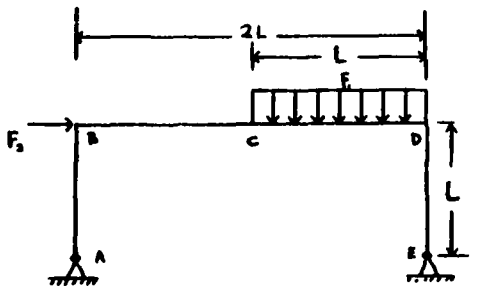

Fig. 5. Frame Under a Distributed and a Concentrated Load.

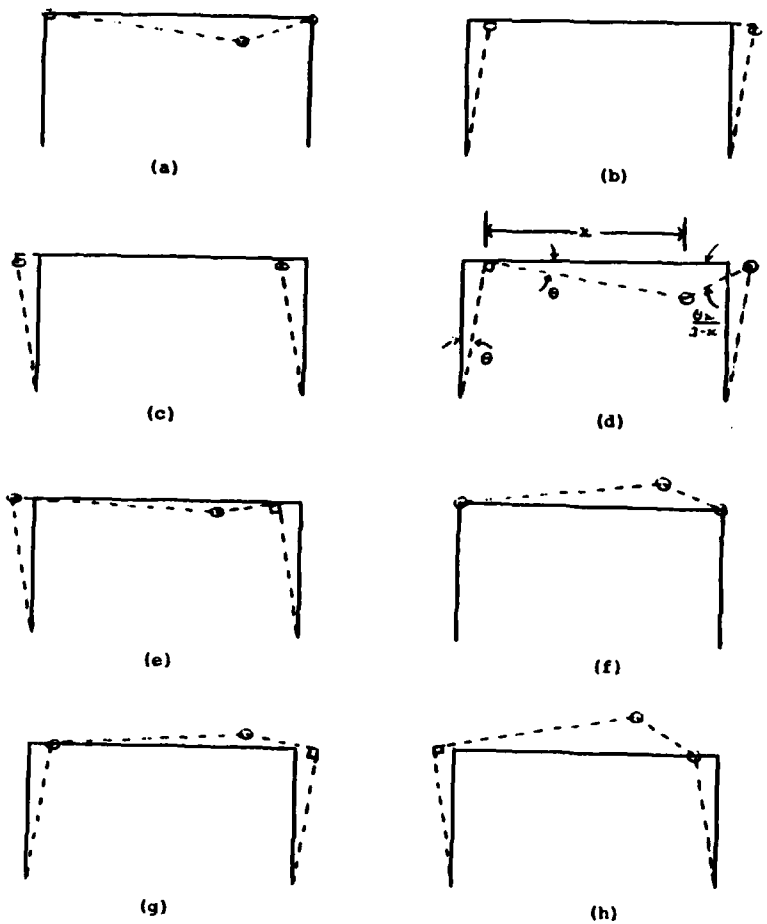

Fig. 6 Collapse Mechanisms for the Frame of Fig. 5.

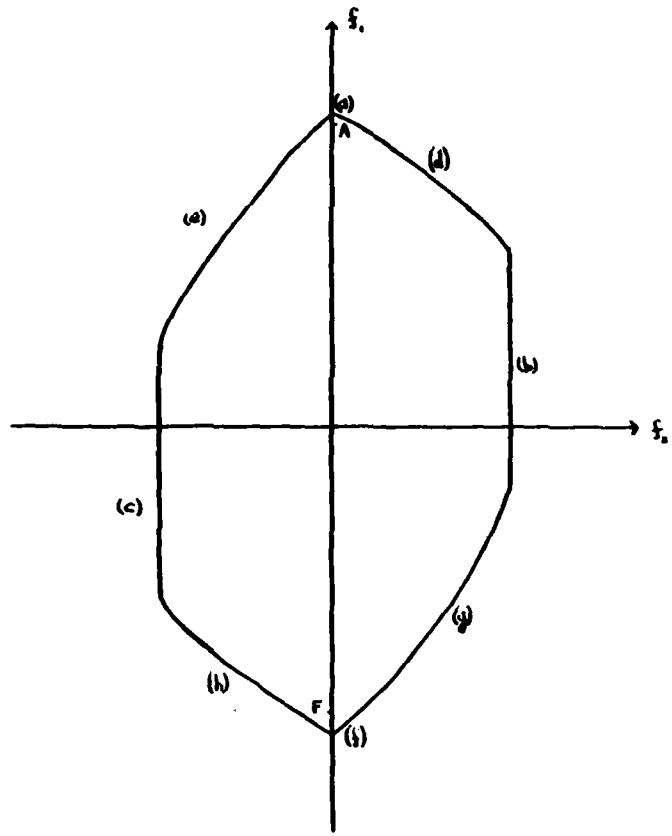

Fig. 7(a). Domain of Loads for the Frame of Fig. 4 for which Instantaneous Plastic Collapse Cannot Occur.

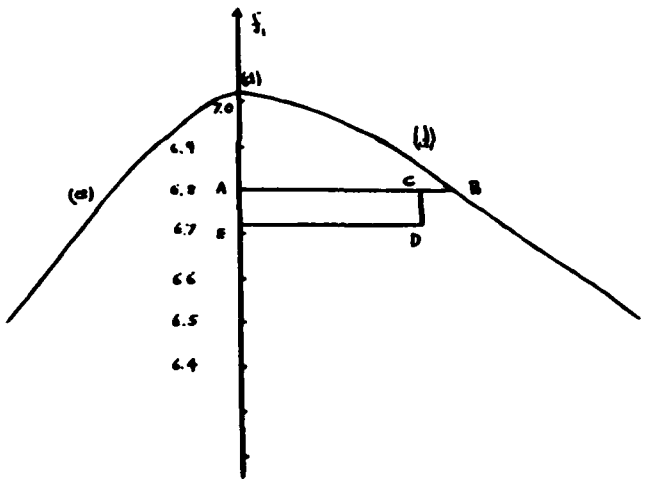

Fig. 7(b). Detail of Fig. 7(a).

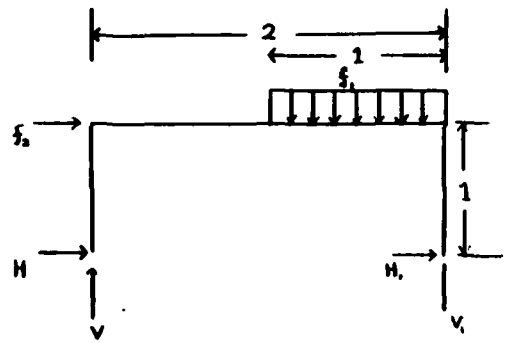

Fig. 8. Free Body Diagram for the Frame of Fig. 5.

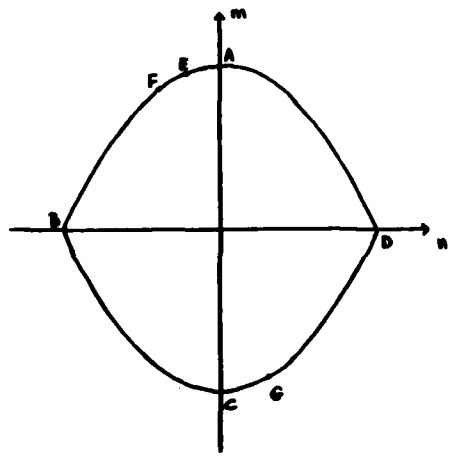

Fig. 9. Interaction Curve for Combined Tension and Bending.

DATE
FILME
7-8